Magnitude of the 39.8 ka Campanian Ignimbrite, Italy: insights from an ignimbrite isopach map

Aurora Silleni[1,2*], Guido Giordano[1], Roberto Isaia[3], Michael H. Ort[2]

[1] Dipartimento di Scienze, Università di Roma Tre, Rome, Italy

[2] SES, Northern Arizona University, Flagstaff, USA, AZ

[3] Istituto Nazionale di Geofisica e Vulcanologia, Osservatorio Vesuviano, Naples, Italy

*** Correspondence:**
Corresponding Author
Aurora.Silleni@nau.edu

Keywords: Campanian Ignimbrite; Campi Flegrei; Isopach maps; Ignimbrite volumes; Pyroclastic density currents; Super-eruption.

Manuscript Length

This manuscript consists of 9084 words, 8 figures and 3 tables.

Abstract

The 39.8 ka Campanian Ignimbrite (CI) is the largest caldera-forming eruption of the Campi Flegrei during the Quaternary, which had a global-scale impact on the environment and human populations. The cooling following the eruption and the several effects of it strongly affected the paleoenvironment and the migration of hominids in Europe. The volume of the eruption is necessary to constrain the climate model of this area in the past. However, despite a large number of studies, the Dense Rock Equivalent (DRE) volume estimates range from 60 to 300 km^3. Here we present a review of the previous volume evaluations and a new calculation of the volume of the ignimbrite. This estimate is constrained by the first total CI isopach map, developed through a method able to reconstruct the paleo-topography during the eruption, which is easily reproducible in all ignimbrites strongly topographically controlled and allows the calculation of well-defined uncertainties. The preserved total bulk extra-caldera volume of the ignimbrite is estimated at 61.5 km^3 ± 5.5 km^3. The total PDC deposit volume is then corrected for erosion, ash elutriation, the intracaldera deposit volume and the volume of tephra deposited in the sea. The total final volume estimate of the eruption ranges from 165 km^3 – 248 km^3 DRE. This value corresponds to a mass of 4.3 - 6.5 x 10^{14} kg, a magnitude (M) of 7.7 and a VEI of 7. This M makes the CI the largest-magnitude Quaternary eruption in the Mediterranean area. The new detailed estimation of CI eruption physical parameters confirms this event has significantly affected human activity and the environment on a large scale at the time of the eruption and, in the future, an event of this size would be cataclysmic.

1 Introduction

Pyroclastic density currents (PDCs) have large impacts on human communities and the environment; they can cause catastrophic environmental and property damage and loss of life, as well as accounting for the major proportion of deaths caused by volcanic activity. In the last 200 years,

26.8% of volcano-induced mortality resulted from PDCs (Tanguy et al., 1998; Witham, 2005). Moreover, global and regional climatic effects can result from the injection of ash and sulfur aerosols into the stratosphere during large explosive eruptions, leading to a "volcanic winter" (Rampino and Self, 1992; Stuiver et al., 1995; Thordarson and Self, 1996). The quantitative computation of the size of explosive eruptions is essential to understand their potential impact on humans, climate and ecosystems (Mason et al., 2004). Calculating the volume of volcanic large eruptions is necessary to define the size and to model the climate effects of these natural phenomena occurred in the past.

The total eruptive product of large caldera-forming eruptions can consist of both fall deposits and ignimbrites (Parfitt and Wilson, 2008), and typically the largest proportion is transported in PDCs and emplaced as ignimbrites. Despite numerical models have greatly improved estimates of tephra dispersal from the fallout phase in recent years (Bonadonna et al., 1998, 2005; Bonadonna and Phillips, 2003; Costa et al., 2006, 2012; Barsotti et al., 2008; Folch et al., 2010; Folch, 2012), a clear "reference" method for the calculation of ignimbrite volume does not exist and uncertainties on such computations are huge (Mason et al., 2004). The volume of ignimbrites was subject of numerous studies (Smith, 1960; Parker and McDowell, 1979; Newhall and Self, 1982; Walker, 1983; Aldiss and Ghazali, 1984; Morgan et al., 1984; Ratté et al., 1984; Henry and Price, 1984; Sparks et al., 1985; Knight et al., 1986; Wilson, 2001; Mason et al., 2004; Lee et al., 2004; Pérez et al., 2006; Geyer and Martí, 2008; Folkes et al., 2011; Crosweller et al., 2012; Best et al., 2013a, 2013b; Brown and Andrews, 2015; Pacheco-Hoyos et al., 2018), however it remains difficult to evaluate due to the irregularity of the ignimbrite surface, the variable thickness (controlled by the paleomorphology), the effect of erosion, the presence of younger products and the variable density of the deposits. The eruptive volume, and as a consequence the ignimbrite volume, is essential for magnitude (M) and VEI computation of an eruption. The total absence of any well-defined quantitative method for the calculation of the volume of ignimbrites, which form the major part of eruption M greater than 5, is one of the main outstanding issues in volcanology (e.g. the collapse caldera database (CCDB) project, Geyer and Martí, 2008; the LAMEVE project, Crosweller et al., 2012).

The lack of a standardized method for the calculation of ignimbrite volumes, which makes most of the existing figures for large volume ignimbrites rather poorly constrained and unreproducible, allows large spans of volumes estimated (e.g. Cerro Galán, Folkes et al., 2011; Campanian Ignimbite, Scarpati et al., 2014). The case of study of this work is the Campanian Ignimbrite (CI; Barberi et al., 1978; De Vivo et al., 2001; Fedele et al., 2008; Fisher et al., 1993), associated with the most powerful caldera-forming eruption from Campi Flegrei (CF) (Fig. 1A) (Rosi and Sbrana, 1987; Perrotta et al., 2006; Scarpati et al., 2013), which occurred at 39.8 ka (Giaccio et al., 2017). It is one of the largest late Quaternary explosive events and has been considered as an example of a super-eruption (Sparks et al., 2005). The CI tephra represents the most widespread volcanic deposit and one of the most important temporal/stratigraphic markers for the Early Upper Paleolithic of western Eurasia (Fedele et al., 2003; Pyle et al., 2006; Giaccio et al., 2008). The eruption may have affected human residents in different ways: by destroying the animal and human populations, by altering the species composition and growth rhythm and by changing the availability of water (Fedele et al., 2002, 2007; Lowe et al., 2012). The abrupt volcanic cooling following the eruption occurred in a more intense way in Eastern Europe and Northern Asia, and reached from -6°C up to -9°C. The cooling could have influenced the migration of the populations and have affected the daily life for Neanderthals and modern humans during the Middle to Upper Paleolithic transition (Black et al., 2015; Marti et al., 2016).

In this work, we present a review of all papers that determined the CI volume. Despite the large number of studies, the estimates of total Dense Rock Equivalent (DRE) volume of CI range from 60

to 300 km^3, with no apparent convergence on an accepted value and none of this report a well-constrained method for the ignimbrite volume, or the associated uncertainties (Thunell et al., 1979; Cornell et al., 1983; Rosi et al., 1983, 1999; Fisher et al., 1993; Civetta et al., 1997; Rolandi et al., 2003; Fedele et al., 2003; Perrotta and Scarpati, 2003; Pyle et al., 2006; Giaccio, 2006; Marianelli et al., 2006; Pappalardo et al., 2008; Costa et al., 2012; Scarpati et al., 2014; Marti et al., 2016). The volume of distal tephra (both Plinian and co-ignimbrite) is well defined due to the many measurements across the vast region and a recent improvement of computational methods (Costa et al., 2012; Marti et al., 2016). Nevertheless, the volume of the PDC deposits was never calculated by direct measurements. We propose a rigorous method to develop, for the first time, a complete isopach map of the Campanian Ignimbrite based on mapping of the preserved deposits and the reconstruction of the paleomorphology, especially in mountain areas, a method which can be easily applied to other ignimbrites in the world. We provide a revised volume of the pyroclastic density current extra-caldera deposits of the CI preserved on land based on a verifiable method of calculation and with the relative uncertainties. Using this as a base, we correct for erosion, elutriation, intracaldera volume and underwater deposits to calculate the most reliable total bulk and Dense Rock Equivalent (DRE) volumes for this eruption. The obtained volume strongly reduces the total error in the previous estimates, which should be used to better develop and constrain the climate model of the Eastern Europe during the Paleolithic period.

2. Volcanological background

The activity in the Campi Flegrei began prior to 80 ka (Pappalardo et al., 1999; Scarpati et al., 2013). The area consists of two nested depressions formed and activated during both the CI and the more recent ~15 ka Neapolitan Yellow Tuff (NYT) eruptions (Orsi et al., 1996; Di Vito et al., 1999; Perrotta et al., 2006; Acocella, 2008; Vitale and Isaia, 2014). A recent study identified an M 6.6 event correlated to the Y-3 tephra, named Masseria del Monte Tuff; this eruption is likely to have generated a caldera collapse between CI and NYT (Albert et al., 2019). After the NYT eruption, intra-caldera volcanic activity continued with more than 70 eruptions, subdivided into three volcanic epochs: epoch I (15-10.6 ka), epoch II (9.8-9.2 ka) and epoch III (4.6-3.8 ka) (Di Vito et al., 1999; Isaia et al., 2009; Smith et al., 2011). The last eruption occurred in 1538 CE and led to the formation of the Monte Nuovo tuff cone.

The CI eruption emplaced both pyroclastic fall and PDC deposits in a complex sequence currently exposed in proximal, medial, distal and ultra-distal outcrops (Fig. 1) (Barberi et al., 1978; Rosi et al., 1988, 1996, 1999; Fisher et al., 1993; Perrotta and Scarpati, 1994, 2003; Orsi et al., 1996; De Vivo et al., 2001; Cappelletti et al., 2003; Perrotta et al., 2006; Fedele et al., 2008b; Engwell et al., 2014; Scarpati et al., 2015a, 2015b; Sparice, 2015; Scarpati and Perrotta, 2016; Smith et al., 2016). The first phase of the eruption generated a Plinian column up to 44 km high (Rosi et al., 1999; Marti et al., 2016), producing a widespread fall deposit dispersed by winds to the east (Rosi et al., 1999; Perrotta and Scarpati, 2003; Marti et al., 2016; Scarpati and Perrotta, 2016). A pyroclastic density current then spread over an area of 7,000 km^2 and surmounted ridges more than 1,000 m high (Barberi et al., 1978; Fisher et al., 1993). This stage caused the caldera collapse and the accumulation of lithic breccia's deposits (Breccia Museo) in scattered outcrops along the caldera rim (Perrotta and Scarpati, 1994; Melluso et al., 1995; Rosi et al., 1996; Fedele et al., 2008b). In distal outcrops, most of the CI is represented by a massive, gray ignimbrite (Barberi et al., 1978; Fisher et al., 1993; Scarpati and Perrotta, 2012; Scarpati et al., 2015a). In more distal and ultra-distal sites deposits are made up by coarse to fine ash containing both co-plinian and co-ignimbrite tephra (Thunell et al., 1979; Sparks and Huang, 1980; Engwell et al., 2014; Smith et al., 2016). The tephra marker related to this eruption is essential to correlate volcanological and archeological sites in the Mediterranean area and Eastern

Europe. Tephra-based correlations of human sites were used to date the Middle to Upper Paleolithic transition (Lowe et al., 2012).

The complex stratigraphy of this eruption differs between proximal and distal outcrops (Fig. 1B, Fig. 1C). Moreover, it is difficult to study the lateral correlations due to the absence of outcrops in medial areas (except for the Lago di Patria outcrop, Table A2 in Data Repository), because all quarry-pits have been refilled. The limited drill core data shows little evidence of lateral unit change. In our study, we refer to the stratigraphic units proposed by Fedele et al. (2008) (proximal area) and Cappelletti et al. (2003) (medial and distal areas). The stratigraphy in proximal areas, from bottom to top, consists of 6 units: 1) Plinian pumice fallout deposit (PPF); 2) unconsolidated stratified ash flow (USAF); 3) welded gray ignimbrite (WGI) interlayered with some more welded levels (Piperno); 4) lower pumice flow unit (LPFU); lithic breccia unit (BU), in places with welded spatter beds (SU); and 6) upper pumice flow unit (UPFU). The stratigraphic sequence of distal outcrops involves, from bottom to top: 1) PPF; 2) USAF; 3) WGI; 4) lithified yellow tuff (LYT); and 5) coarse pumice flow (CPF).

3. The previous estimates of the CI volume

Defining the eruptive volume is necessary to simulate the climate impact of this eruption in Eastern Europe. Here is reported a review of the previous estimates of the CI volume aim to define a constrained volume for this eruption (Table 1).

The total volume erupted during a caldera-forming eruption, like the CI, is composed of the mass ejected during the phases that produced Plinian columns (V_{pf}), and pyroclastic density currents (V_{pdc}) (1):

$$\boldsymbol{V = V_{pf} + V_{pdc}} \quad (1)$$

Both V_{pf} and V_{pdc} are made of the main primary deposits (respectively the Plinian fallout V_{ppf}, the proximal pumice lapilli deposit, and the ignimbrite V_i) and their associated co-plinian fall (V_{cpf}) and co-ignimbrite ash fall (V_{ci}). Indeed, fine ash suspended in the atmosphere can be co-plinian rather than co-ignimbrite (Fierstein and Hildreth, 1992). Consequently (2):

$$\boldsymbol{V = V_{ppf} + V_{cpf} + V_i + V_{ci}} \quad (2)$$

Due to the difficulty to distinguish the contribution of the co-plinian fall and the co-ignimbrite ash fall in ultra-distal locations, some authors simply refer to the widespread Y-5 ash layer, which comprises both (Table 1). This layer is the tephra marker linked to the CI eruption and is recognized from marine cores across the Eastern Mediterranean region to Russia, for this reason, Y-5 is an excellent chronostratigraphic marker in the Northern Hemisphere (Thunell et al., 1979; Cornell et al., 1983; Narcisi and Vezzoli, 1999; Ton-That et al., 2001; Fedele et al., 2003; Giaccio et al., 2006; Pyle et al., 2006; Engwell et al., 2014; Smith et al., 2016). Previous studies distinguished also the co-plinian and co-ignimbrite contribution (Sparks and Huang, 1980; Perrotta and Scarpati, 2003; Marti et al., 2016; Smith et al., 2016); some of them calculated the relative volumes (Perrotta and Scarpati, 2003; Marti et al., 2016).

The first volume estimate of the ignimbrite was presented by Thunell et al. (1979). Based on a geometrical method that considers a covered area of over 6000 km^2 with a thickness up to 100 m and assuming a radial flow of the PDC, they estimate the DRE volume is at least 30-40 km^3. The DRE volume of the Y-5 ash layer within the 1-cm isopach contour was also estimated at 30-40 km^3 (65

km^3 bulk) and the authors recognized that Y-5 is composed by a co-plinian and a co-ignimbrite ash, but they did not calculate each contribution to the volume. Their total DRE volume is 60-80 km^3 for the eruption.

Cornell et al. (1983) calculated the ash-fall layer volume of Y-5 from an isopach map derived by different cores drilled in the Mediterranean Sea (73 km^3 bulk). They then included the ignimbrite DRE volume proposed by Thunell et al. (1979) in their overall eruption volume estimate. On the other hand, the bulk volume of the original pyroclastic current was estimated by Fisher et al. (1993) of about 500 km^3 by circumscribing a circle of deposits with a radius of 100 km, 100 m thick at the center that thinned to zero at the perimeter of the circle.

Civetta et al. (1997) is one of the first works that subdivided the volume of the CI based on the pumice composition. The authors divided the magma into three different types: a most evolved one that consists of Plinian fallout and some ignimbrite up to 50 km from the vent (a volume of 25 km^3 DRE), a magma with intermediate composition that includes some of the ignimbrite out to its farthest extent (100 km^3 DRE), and a least-evolved magma that includes much of the ignimbrite in the Campanian Plain (20 km^3 DRE). All the volume calculations were made by circumscribing circles with a radius similar to the maximum distance reached from the vent by that magma type and a thickness that goes from the maximum thickness of ignimbrite of that composition at the caldera center to zero at the perimeter of the circle.

Pappalardo et al. (2008) used petrological data to constrain the pre-eruptive magma storage dynamics and, in agreement with Civetta et al. (1997), proposed a total volume of 200 km^3 DRE (20 km^3 for the fallout and 180 km^3 for the ignimbrite).

Rosi et al. (1999) calculated the bulk volume of the Plinian fallout as 15 km^3 based on the method proposed by Pyle (1989), which assumes exponential thickness decay away from the vent and an elliptical isopach distribution with the source at one focus; in the CI case, this focus corresponds to a central vent, located in the Campi Flegrei caldera center (town of Pozzuoli). The same technique was used by Perrotta and Scarpati (2003), who estimated a bulk volume of about 4 km^3, the different value being the result of a different way than Rosi et al. (1999) used to trace the isopach lines. In the same work (Perrotta and Scarpati, 2003), the authors attempt, for the first time, to discriminate, in term of volumes, between the co-plinian and co-ignimbrite components. The coarse ash of ultra-distal deposits was interpreted as the co-plinian phase, while the fine ash represents the co-ignimbrite component. The authors evaluated the thicknesses of the two parts and estimated the volume as follows: 16 km^3 of co-plinian ash and 100 km^3 of co-ignimbrite ash. Scarpati and Perrotta (2016) subdivided the fallout into five layers (A to E) and calculated the volumes for each of them using the same exponential fitting, obtaining a primary fallout of about 5 km^3 (~1 km^3 DRE) and a co-plinian ash of about 15 km^3 (~7 km^3 DRE).

These analyses were improved consequent to Pyle et al. (2006), who estimated the minimum bulk volume of the CI fallout of 74 km^3 or 31 km^3 DRE: the authors used the general observation that many fallout deposits show exponential decay of thickness (Pyle, 1989). In the same work, the authors compared these results with a second approach based on the rate of thinning of the distal ash sheets (Pyle, 1989, 1990): given that the thickest ash layer in marine cores is of the order of 10–20 cm, it is most likely that the total bulk ash volume associated with the eruption was in the range 74-120 km^3 (31–50 km^3 DRE) (Pyle et al., 2006).

A first attempt to compare all the volume estimates was proposed by Fedele et al. (2003), who considered the sum of the conservative estimates reported in literature. The total DRE volume they proposed is 200 km^3 (the sum of the fallout, the PDC deposits and the Y-5 ash layer volumes (Thunell et al., 1979; Civetta et al., 1997; Rosi et al., 1999)). Similar value was proposed by Giaccio (2006), 215 km^3 DRE (385 km^3 bulk), he calculated the volume of the PDC using a complex truncated cone, with a concave surface and variable heights: 70 m up to 10 km from the center, 50 m up to 20 km, 20 m up to 45 km and 0 m up to 100 km. At the same time, he proposed a revised isopach map for the fallout deposits, resulting in a volume estimate of 10 km^3 (3 km^3 DRE). Moreover, combining all available data on the distal tephra of CI from the literature (Cornell et al., 1983; Melekestsev et al., 1984; Paterne et al., 1986; McCoy and Cornell, 1990; Castagnoli et al., 1995; Seymour and Christanis, 1995; Narcisi and Vezzoli, 1999; Ton-That et al., 2001; Upton et al., 2002; Seymour et al., 2004), Giaccio (2006) calculated the volume of this fraction as 180 km^3 (86 km^3 DRE) and thus estimated a bulk volume of 575 km^3 (300 km^3 DRE).

The most difficult part of drawing isopach maps of the Plinian fallout is the limited number of distal subaerial locations where the tephra is found. To solve this, a new volume estimate was proposed by Costa et al. (2012) based on the fit of an advection – diffusion tephra dispersion model to thickness data. They obtained a bulk volume of the tephra of 250-300 km^3 (104-125 km^3 DRE) and a total volume of the eruption of 430-680 km^3 (180-280 km^3 DRE).

Scarpati et al. (2014) estimated the PDC volume applying equation (3) assuming a co-ignimbrite volume (V_{ci}) of 100 km^3 obtained by Perrotta and Scarpati (2003) and a mean vitric loss of 0.65. The method is based on the enrichment factor of Walker (1972, 1980) and the vitric loss of the ignimbrite proposed by Sparks and Walker (1977). The volume (V) (3) is equal to:

$$\boldsymbol{V = \frac{V_{ci}}{vitric\ loss} - V_{ci}} \quad (3)$$

This method is strongly influenced by the mean value of vitric loss used, which is normally estimated from sporadic punctual measurements. The bulk volume of the PDC deposits thus estimated is 54 km^3 (25 km^3 DRE, using a density of 2600 kg/m^3). In the same study, the authors proposed a review of the previous volume estimations (Scarpati et al., 2014).

The most recent work on the fallout volume was presented by Marti et al. (2016). The authors recognized two distinct plume phases: the Plinian (V_{pf}) and the co-ignimbrite fall. They applied a computational inversion method that explicitly accounts for the two phases and for gravitational spreading of the umbrella cloud, dividing in two phases provide the best estimate, as they are two different spreading and source phenomena. The Plinian fallout bulk volume thus calculated is 54 km^3 (22.6 km^3 DRE, using a density of 2500 kg/m^3) and the co-ignimbrite bulk volume is 153.9 km^3 (61.6 km^3 DRE), for a bulk total volume of 207.9 km^3 (84.2 km^3 DRE).

To summarize, the existing estimates of the total DRE volume of the CI eruption range from 60 to 300 km^3 (Thunell et al., 1979; Cornell et al., 1983; Rosi et al., 1983, 1999; Fisher et al., 1993; Civetta et al., 1997; Rolandi et al., 2003; Fedele et al., 2003; Perrotta and Scarpati, 2003; Pyle et al., 2006; Giaccio, 2006; Marianelli et al., 2006; Pappalardo et al., 2008; Costa et al., 2012; Scarpati et al., 2014; Marti et al., 2016) and those for the bulk volume of the CI pyroclastic density current deposits range between 54 and 500 km^3 (Thunell et al., 1979; Cornell et al., 1983; Fisher et al., 1993; Civetta et al., 1997; Rolandi et al., 2003; Marianelli et al., 2006; Pappalardo et al., 2008; Scarpati et al., 2014). The margin of error in these volumes is unacceptably high due to the different methods used, especially in view of the relevance of such figures on the impact on climate and the environment.

While the computational methods for the fallout deposits have improved significantly in the past ten years and the related figures for the CI fallout phase appear strong and solidly based on field data (Costa et al., 2012; Marti et al., 2016), the volume figures for the CI ignimbrite appear to remain very poorly constrained and without well-assessment uncertainties. Although this volume largely affects the estimation of the volume of elutriated co-ignimbrite ash, which is the dominant fallout phase across Europe and the most relevant fraction of ash injected into the stratosphere at the time of the eruption (e.g. Costa et al., 2018).

4. Constructing the CI isopach map

In order to reduce this wide range in volume estimates, we focus on constraining the volume of the PDC deposits of the CI. Our calculation of thickness and volume does not take into account the initial pyroclastic Plinian fall phase and the co-ignimbrite fallout; we used the fall volume calculation of other authors, the maximum and the minimum proposed in literature by Perrotta and Scarpati (2003) and Marti et al. (2016). Our CI isopach map is based on previous published data, fieldwork and the assessment of the paleo-topographic control exerted on the deposits thickness distribution.

4.1 *Database and fieldwork*

Published data regarding CI thickness and outcrop locations were collected from 42 papers (presented in Data Repository, Table 1). The whole data were inserted in a GIS Open-Source QGIS 3.4 (https://www.qgis.org/it/site/) database including 238 localized outcrops. The database includes the name of the location, the lithological description, the geographic coordinates, the elevation a.s.l., the thickness of the flow units (specifying whether total or outcrop thickness), the maximum lithic dimensions and the degree of welding. Where both base and top of the CI are exposed, the thickness is classified as total and elsewhere it is considered a minimum thickness.

This database has been augmented by our field data acquired in 97 locations (presented in Data Repository, Table 2), both in proximal and distal areas (Fig. 1D). Fieldwork was aimed to measure the total or minimum thickness, the local stratigraphy and to understand the relation of the ignimbrite with the topography.

4.2 The zero-thickness isopach

The zero-thickness isopach is an outer limit beyond which the CI is not present, and it delimits the current areal distribution of the PDC outcrops. The isopach was reconstructed through a first phase of revision of the geological maps already existing at the scale 1:10,000, 1:50,000 or 1:100,000 (Servizio Geologico d'Italia, 1963, 1965a, 1965b, 1965c, 1966, 1967a, 1967b, 1971a, 1971b, 1975; Rosi and Sbrana, 1987; Vezzoli and Barberi, 1988; ISPRA, 2009, 2010, 2011a, 2011b, 2011c, 2011d, 2014a, 2014b, 2016, 2018; Sbrana and Toccaceli, 2011). The contact was traced between the CI and older units and extrapolated where CI does not crop out. In this circumstance, the ignimbrite is generally covered by younger deposits, but it is necessary to assess if the CI was never emplaced there. To distinguish between these two cases, a statistical and morphological analysis of the actual slope of the top of the CI was applied and a comparison between the topography and the average slope of the CI top was carried out. Where the slope angle is comparable, the area was included in the zero-thickness isopach, even if CI is not cropping out. Greater slope angles were attributed to underlying basement (mostly Meso-Cenozoic calcareous or flysch) and the isopach was traced to leave out these areas and no primary CI deposition was interpreted.

4.3 The isopachs

To determine the isopach locations, two different methods were used, one in the proximal area (from the caldera to the base of the Apennine Mountains, including the Campanian Plain) and one in the more distal area. The almost complete lack of outcrops in the Campanian Plain and the valley-ponded depositional style in the ridge-valley topography of the Apennine Mountains (Rosi et al., 1983, 1996; Perrotta et al., 2010; Langella et al., 2013; Scarpati et al., 2014, 2015a; Sparice, 2015; Fedele et al., 2016) make these different approaches necessary.

In the proximal area, data from the literature (Bellucci, 1994; ISPRA, 2011d; Milia and Torrente, 2007; Ortolani and Aprile, 1985; Rolandi et al., 2003; Scandone et al., 1991; Torrente et al., 2010), consisting of more than 300 thickness values of CI from boreholes, outcrops and geological sections were used to fit isopachs on the map. In the distal area, the isopach locations were based upon our field observations and the reconstruction of the pre-CI topography (Fig. 2). A series of profiles (~ 150) in the Apennine Mountains were drawn to outline the trend of the valleys (Fig. 2B). The coast-line in Mediterranean Sea at the time of the CI emplacement (39.8 ka) was lower than present-day, but it is difficult to define the precise level due to the high tectonic activity in the region and the difference in behavior between a closed basin such as the Mediterranean Sea and the Atlantic Ocean, which responded predictably to global sea-level changes. Based upon limited sea-level correlation work in the Mediterranean basin (Lambeck and Bard, 2000; Antonioli et al., 2004; Antonioli, 2012), we assumed a sea level between 75 m and 87 m lower than present-day.

Topographic cross-sections were traced orthogonally to the center of the valley and to the contour lines, including the flanks of the reliefs and the zero-thickness isopach. The slopes of the valley above the CI zero isopach were extended and gradually shallowed toward the valley center in order to reconstruct the paleo-valley with an inclination of the sides similar to the current slope, always taking into consideration the geological and morphological features (Fig. 2C), and assuming that the Meso-Cenozoic mountain slopes have not significantly changed since 40 ka. This method considers that the CI typically has a valley-pond geometry inside the Apennine Mountains (Rosi et al., 1996; Perrotta et al., 2010; Scarpati et al., 2014, 2015a; Sparice, 2015; Fedele et al., 2016). The base elevation of the paleo-valleys is constrained by field data where the CI base has been measured.

These reconstructed valleys culminate generally in a V shape, with the bottom elevation, above the sea level, for each profile representing the paleo-valley floor. All these elevations represent the ancient pattern of the valley bottom, for this reason, they were modified if they were inconsistent with the progressive downslope decrease in elevation. We also took into account the slope of the present-day drainage network (Fig. 2A).

Finally, the neo-incision of rivers in the profiles was flattened, to not include in the result the linear erosion of the last 39.8 ka (Fig. 2C). The CI thickness is calculated by these modified profiles, and it is always constrained by field data on the CI thickness and with the geological maps. These thickness values are then reported on the isopach map.

All the isopachs were traced always in coherence with field data, for both thickness and base elevation, geology of Meso-Cenozoic sides of the valleys and, finally, the progressive downslope decrease in the base elevation of the valleys referred to the present-day drainage network. Where these data were not consistent, an adjustment in some profiles was necessary. The most significant adjustments were made for a resulting over-thickening inside the valleys. In these cases, the thickness was modified in coherence with fieldwork.

5. Results

We use, as starting point for the volume estimation, the PDC volume, obtained from the detailed isopach map. From the previous review, it is evident that this information lacks in previous works on the CI volume, as a total isopac map. Here, we refer to all PDC units of the CI, that in the medial and distal outcrops are mainly composed by WGI. Density and porosity data are used to define the DRE volume.

5.1 The isopach maps

The statistical and morphological analysis of the upper surface of the CI used 48804 points throughout the areal extension of the deposits (both in proximal and distal areas). This analysis shows that 64% (31057) of the points have slopes lower than 5°. Moreover, 80% of the points have slopes lower than 10° and 99% have a surface slope lower than 55° (Fig. 3). This is in agreement with the observation on the slope of the top surface of the valley-ponded Taupo Ignimbrite, which is around 8° (Wilson and Walker, 1985).

Based on these results, the 0-m isopach was traced to enclose all the mapped CI and areas that probably have the CI below the recent sedimentary cover and have a slope less than 15°. The total area enclosed by the 0-m isopach of the CI is 3216 km^2 (Fig. 4). To understand also the total area of the region involved in the PDC, a shape was drawn comprising all the areal extension of the isopach 0-m. The enveloped area is equal to 7547 km^2, similar to the 7000 km^2 earlier estimate (Barberi et al., 1978).

The isopach map traced in the proximal area does not include the intracaldera deposits. The maximum thickness in proximal areas is 80 m (Fig. 5), mainly based on outcrops near the caldera rim; the CI thins gradually away from the caldera margin. Two areas of thickening are identified just north of the caldera and east of Lago Patria (up to 70 m) and in the area of Casoria (up to 50 m) (Fig. 6A). Three main areas of thinning (down to 10 m) are recognized to the north in the Campanian Plain (Fig. 6B), in the area between Aversa and Acerra and in the south of the Campanian Plain (Fig. 6A).

Two thickened portions are on the northern side of the Campanian Plain (north-east of Mondragone) (Fig. 6B) and on the eastern side (from Caserta to Maddaloni) (Fig. 6C), both just in front of the first Apennine ridges.

The isopach for the distal reaches has a maximum thickness of 50 m in the area of Maddaloni Valley (Fig. 6C). A series of confined valleys show local thickening. These include, from northwest to southeast, Mortola (up to 30 m), Roccamonfina (up to 30 m) (Fig. 6D), San Lorenzello and all the Volturno plain (up to 20 m) (Fig. 6E), Sant'Agata dei Goti (up to 40 m), Tufara (up to 20 m), Monteforte Irpino and Avellino (up to 30 m) (Fig. 6F), Tramonti (up to 10 m) and Sorrento (up to 20 m) (Fig. 6G).

5.2 Density of the CI deposits

More than 40 samples from different outcrops scattered around the Campanian Plain were analyzed to determine their density. Samples were cut in cylinders (with radius between 0.9 cm and 2 cm and height between 0.8 and 5.7 cm) or cubes (sides from 0.8 to 2.5 cm) and analyzed using a Micromeritics AccuPyc II 1340 helium pycnometer. The resulting density was used to interpret total and open porosity, the density is used to determine the DRE volume.

The bulk density (ρ) of the WGI samples from the Campanian Plain ranges from 745 ± 15 kg/m^3 to 1330 ± 3 kg/m^3, these values follow a Gaussian distribution with an average at 980 ± 11 kg/m^3. The bulk density of the Piperno unit ranges from 1275 ± 8 kg/m^3 to 1302 ± 2 kg/m^3, with an average of 1287 ± 4 kg/m^3 (presented in Data Repository, Table 3). Open porosity was estimated with geometric (V_g) and matrix volume (V_{mx}): $100*(V_g-V_{mx})/V_g$, while closed porosity was determined using the DRE of the WGI and Piperno powder, which was obtained by the pycnometer. The total WGI porosity (φ_t) was calculated directly adding up closed and open porosity and it ranges from 49 ± 5% and 71± 5% and the average is 61.6% ± 5%, for the Piperno unit it is 50 ± 1%. The ρ DRE is 2607.7 ± 31 kg/m^3. The DRE volume is determined multiplying the bulk volume by $(100- \varphi_t)/100$.

5.3 Deposits volume calculation

The area enclosed by each isopach, reported in Fig. 7, allows the ignimbrite volume to be calculated. This is the subtended area of the plot thickness-cumulative area (Walker, 1980, 1981); the area of each isopach was calculated directly from the QGIS software. Table 2 displays the values of the area and the volume for each isopach. The largest part of the volume is relative to deposits thicknesses <10 m (60.52%), which is present both in proximal and distal areas, whereas the isopachs from 40 m to 80 m contain less of the 10% of the total volume (7.17%). Summarizing all the isopachs volume, the total volume of the preserved extra-caldera CI deposits on land is 61.5 km^3 ± 5.5 km^3 (22.0 ± 2.2 km^3 DRE).

To understand the extra-caldera volume subdivision in proximal and distal areas, the isopach map is portioned in two parts, one comprising all the Campanian Plain, and the other from the first Apennine ridges to the final runout (Fig. 5). The resulting extra-caldera volumes are 46.4 ± 1.6 km^3 in the proximal area (~75%) and 15.1 ± 3.9 km^3 in the distal area (~25%); the sources of error and the uncertainties were calculated separately for the two methods, their calculation is explained in the Supplementary Material.

A recent study proposed contour maps of the lower and the upper surfaces of the CI for the north-western sector of the proximal area, based on 1000 of lithostratigraphic logs from boreholes (Ruberti et al., 2020). The difference of the upper surface and the lower one is the CI thickness, which is not reported on the work of Ruberti et al. (2020). The extrapolated thicknesses from the maps were compared with the isopach map of the proximal area of this work and it shown great similarities in the areas of Mondragone, Caserta and Lago Patria. On the other hand, there are some differences of the thicknesses in the Volturno Plain, where the authors suggest a thicker CI (Ruberti et al., 2020). To evaluate these discrepancies, a new proximal isopach map was drawn taking into consideration the new thickness data. The volume related to this map is 46.7 km^3, meaning a difference of 0.3 km^3 with the volume previously estimated. This value (0.3 km^3) is fully included in the 1.6 km^3 of error and uncertainties in the proximal area. For this reason, the data proposed by Ruberti et al. (2020) were not inserted in the isopach map reported in this work, however, a greater thickness in the Volturno Plain could be considered, even though it does not change the final total volume of the proximal area and of all the CI.

6. The volume of the Campanian Ignimbrite

The isopach map is essential both to calculate the eruptive volume and to understand the flow dynamics in the interaction with the paleo-topography (Giordano and Doronzo, 2017). The preserved volume of the deposits of an eruption is the first essential datum to understand the magnitude of the eruption itself. These data are generally very poorly constrained for very large explosive eruptions,

mainly due to the difficult to estimate the PDC volume deposits and the areal distribution of the very distal tephra layers.

6.1 Extracaldera volume

Our quantitative evaluation of the CI extra-caldera bulk volume (V_{pr}), is 61.5 km^3 ± 5.5 km^3. The error and uncertainties are in total less than 10%, a good value considering that many published estimates of eruption volume may be barely more precise than an order of magnitude (Mason et al., 2004). This volume is not the total volume of the CI PDC deposits, which depends upon several corrections that must be applied to this value. A significant amount of pyroclastic material was deposited in the sea and within the caldera, significant erosion has occurred in the last 39.8 ka, and a large amount of co-ignimbrite ash elutriated or rose into the air as a column.

The reconstructed isopachs do not consider the linear erosion due to river incision of the CI so the possible areal erosion must be calculated. The linear erosion is referred to the selective erosion due to rivers, while the areal erosion comprises all the regional processes that occurred in the area. The deposits of WGI show a mainly valley-ponded deposit pattern; in many areas where the ignimbrite was deposited in narrow valleys (for instance near Roccamonfina), the only unit that mantles the topography is USAF, while the upper surface of WGI is mainly horizontal (Fig. 3) (Sparice, 2015). This suggests that USAF is a facies emplaced in a wider area distribution than WGI, comprising also topological highs with mantling features. The thickness of USAF is mainly between 10 cm and 1 m and, in rare cases, it can reach 3 m (Fedele et al., 2016). A median thickness of 1 m is assumed as eroded material for all the enveloped area (7547 km^2, projected area) not covered by valley-pond facies, as a reference for the areal erosion. From a DEM, the real surface enveloped area was computed at 9575 km^2, meaning the calculation of the area on the DEM and not on a projected horizontal surface, it was so evaluated also the deposition on mountain slope (as a mantling feature deposition). The volume associated with the areal erosion is 9.6 km^3 (V_e) (3.7 km^3 DRE, using the average density of WGI). This is a correction based on field observation (USAF able to mantling the topography) and an average calculation (the thickness and the area), obviously, it is just a reference value, and could vary if the eroded thickness, or involved area, are considered substantially different.

The CF caldera is located near and below the current sea-level but, about 40 ka, the coastline was farther to the west and south corresponding to a level between 75 and 87 m below its present position (Lambeck and Bard, 2000; Antonioli et al., 2004; Antonioli, 2012) (Fig. 8). Based on the distribution on land of the ignimbrite, safely assumed with a radial spreading (Thunell et al., 1979; Fisher et al., 1993; Ort et al., 2003), and the position of the CF caldera relative to the coastline (Fig. 8) a roughly equal amount of material should be present both on land and offshore (Barberi et al., 1978). The bathymetry offshore shows depressions and valleys right south of the caldera that can be easily areas of ignimbrite deposits accumulation (Fig. 8). Flow deposits of Kos and Krakatau demonstrate that PDC can travel considerable distance above sea water (Carey et al., 1996; Allen and Cas, 2001; Dufek and Bergantz, 2007) as well the Campanian PDC flowed over the water of the Bay of Naples to deposit on the Sorrento Peninsula (~ 35 km from Pozzuoli Bay to Sorrento) (Fisher et al., 1993). As the PDC passed over the water, the more dilute upper parts did not interact with the water while the denser undercurrent developed a sheared contact with the water, leading to pyroclastic material entering the water and developing submarine currents (Dufek et al., 2007).

The presence of the turbidity currents in the Mediterranean basin and coeval to the eruption was confirmed by the analyses of the core CT85-5 in the Tyrrhenian Sea (40°19’02’’N, 11°15’42’’E) located more than 200 km west from the CF caldera (Castagnoli et al., 1995; Giaccio, 2006; Giaccio

et al., 2006; Hajdas et al., 2011). The CI tephra recognized within the core was used as an important time marker and it is 45 cm thick. The nearby CT85-6 confirmed the presence of the CI tephra, however, it was less studied as its record is shorter and the CI is not reported fully (Hajdas et al., 2011). In the CI layer, were found shallow water gastropods and internal lamination, which indicate that at least 10 cm of the section are from turbiditic origin (Castagnoli et al., 1995; Giaccio, 2006; Hajdas et al., 2011). These volcanoclastic currents related to the CI eruption are strongly reported in all the Tyrrhenian basin (Giaccio, 2006; McCoy and Cornell, 1990) interpreted as a large syn-eruptive phenomena of the CI deposits, triggered by the PDCs which entered inside the water and in general to the volcanic event. The turbidity currents can be reasonably considered as primary products of the eruption (Giaccio, 2006).

For these reasons a large amount of underwater material is realistic and, because of the nearly equal radial area covered by sea versus on land, is considered equal to the on-land material, so each is considered to have a volume of 61.5 $km^3 \pm 5.5$ km^3 (V_m).

6.2 Intracaldera volume

Some deep wells were drilled in the 1940s and 1950s to understand the deep geothermal system in the Campi Flegrei, reaching depths of 1600-3000 m below ground surface (Rosi and Sbrana, 1987). A well-developed neogenic mineral zonation was observed with four main zones marked by distinctive mineral assemblages: argillitic zone (down to ~700 m), illite-chlorite zone (down to ~1300 m), calc-aluminum silicate zone (down to ~2300 m) and thermometamorphic zone (below ~2300 m). The temperatures reach high values of 360°C in the calc-aluminum silicate zone (Rosi and Sbrana, 1987). These wells reached also the CI, but the extensive hydrothermal alteration prevented its identification. Due to the high uncertainties of correlating CI deposits inside the caldera, the isopach map was traced without the intracaldera area and the intracaldera volume was not estimated in this work, which refers to literature data.

More recently, a 506 m drill-hole has been drilled western of Naples, reaching both NYT and CI (De Natale et al., 2016; Mormone et al., 2015). The hydrothermal alteration in proximity of CI (around 439 and 501 m) was recognized and made the correlation with the deposits extremely difficult. However, through lithological, mineralogical and $^{40}Ar/^{39}Ar$ dating the authors recognized at least 250 m of intracaldera CI (De Natale et al., 2016), this value was already observed through geological and geophysical features (Torrente et al., 2010). The ignimbrite volume inside the caldera, which in this work has a dimension of 64 km^2, was then estimated less than 16 km^3 (De Natale et al., 2016).

Though, from field observation and literature data (De Natale et al., 2016), there is no evidence of significant intracaldera thickening. Therefore, a very large (~0.9) *f* value (the fraction of the total magma volume erupted prior to the onset of collapse) is attributed to the CI eruption (Cashman and Giordano, 2014). Additionally, the ratio between the measured collapses related to the NYT and CI is 2.5, a data that looks unreliable due to the much larger volume of CI than the NYT (De Natale et al., 2016). The authors proposed two models to explain the low intracaldera thickening: a vent outside the Campi Flegrei caldera (model 1) and a very large regional uplift related to the CI eruption (model 2). The second model seems realistic to explain the anomalous ratio, especially if a much smaller eruption as Monte Nuovo one (with a volume less than 1 km^3 DRE (D'Oriano et al., 2005; Piochi et al., 2005)) produced an uplift of 5 to 8 m (Capocci, 1835; Pescandola, 1947).

There are some uncertainties due to the caldera dimension, indeed, Vitale and Isaia (2014) proposed a polygonal caldera 12 km wide, which corresponds to an area of 144 km^2. Considering an average

thickness of 250 m of intracalderic deposits (De Natale et al., 2016), and an area varying from 64 to 144 km^2, the intracaldera volume (V_{intr}) ranges between 16 km^3 to 43.2 km^3 (7.9-21.4 km^3 DRE).

6.3 Distal tephra volume

The CI tephra is an important correlation tool and time marker mainly to relate the Quaternary stratigraphy in different basins and archeological sites in the Western Eurasia. The tephra layer is visible in numerous sedimentary records, including archeological (Kozlowski, 1998; Fedele et al., 2003; Pyle et al., 2006; Anikovich et al., 2007; Giaccio et al., 2008), marine (Keller et al., 1978; Paterne et al., 1986, 1999; Ton-That et al., 2001), and terrestrial sequences (Veres et al., 2013) as also cave-entrance environments (Fedele et al., 2003; Giaccio et al., 2008) and lacustrine records (Narcisi, 1996). In very distal sites, it can be found as a cryptotephra not visible to the naked eye, but clearly useful as an absolute and relative chronological and stratigraphic marker (Lowe et al., 2012). The tephra it has been identified in the Mediterranean basin (Thunell et al., 1979; Sparks and Huang, 1980; Cornell et al., 1983; Paterne et al., 1986, 1988, 1999; Cramp et al., 1989; Vezzoli, 1991; Calanchi et al., 1998; Ton-That et al., 2001), in south-western Romania (Veres et al., 2013), in Italy (e.g. Monticchio, Fedele et al. 2002, 2003; Giaccio et al. 2008; Narcisi 1996), in Eastern Europe and Russia (Melekestsev et al., 1984; Pyle et al., 2006; Anikovich et al., 2007), in Greece (Vitaliano et al., 1981; Seymour and Christanis, 1995; Kozlowski, 1998), in Ukraine (Melekestsev et al., 1984) and in Bulgaria (Harkovska et al., 1990; Bluszcz et al., 1992; Paterne, 1992).

Defining the distribution of the ultra-distal deposits is a difficult task due to the limitation of the field data available and to the thinning of the ash layers, affected by a large erosion. Underestimation of the deposit volume can be derived by simple extrapolation from proximal, medial and distal data to the ultra-distal region. The case of the CI is complicated by the presence of both co-plinian ash and co-ignimbrite ash due to the large-volume pyroclastic flow that generate a co-ignimbrite plume (Woods and Wohletz, 1991; Woods, 1998), both transported far away from the vent up to eastern Europe and Russia (Thunell et al., 1979; Cornell et al., 1983; Narcisi and Vezzoli, 1999; Ton-That et al., 2001; Fedele et al., 2003; Giaccio et al., 2006; Pyle et al., 2006; Engwell et al., 2014; Smith et al., 2016).

The ultra-distal tephra volume is necessary to define the total CI eruptive volume. Sparks and Huang (1980) recognized the bimodal grain-size of the ultra-distal deposits of the CI, where the coarse lower unit is formed during the plinian phase, while the finer unit at the top corresponds to the co-ignimbrite phase, features observed also by Wulf et al. (2004) in the Monticchio Lake. Sparks and Huang (1980) estimated that the fine layer represents, on average, the 65% of the tephra volume, which increases away from the vent, from 20% at 450 km distance up to 95% of the deposit at 1660 km from the vent. However, an absolute volume for each phase was not defined. The decreasing of Plinian material with distance from the source was also observed by Engwell et al. (2014), who used the grain-size data to investigate the dispersal of the co-plinian and the co-ignimbrite phases. The authors calculated that $40 \pm 5\%$ of the volume of tephra within 850 km of the vent is related to the Plinian phase. Furthermore, they recognized the difficult to quantify the absolute volume of the two phases.

The first work that attributed a volume to the two components was presented by Perrotta and Scarpati (2003). The method used by the authors was previously explained. At a later time, Marti et al. (2016) modelled the CI tephra dispersion and gave a volume estimation of the two phases. They recognized the great impacts of the tephra fallout in the westward migration of modern hominid groups in Europe.

Smith et al. (2016) used the CI tephra glass composition to map the dispersal of the Plinian and the co-ignimbrite components over the dispersal region. This method is substantially crucial to recognize the CI in the ultra-distal region. In an especial way, it is essential to correlate this important chronological marker in archeological sites and to investigate spatio-temporal variability in climate change and the timing of human cultural events in eastern and central Europe (Fedele et al., 2003, 2008a, 2008b; Lowe et al., 2012). Based on the glass composition, the authors recognized that the PDC component is dominant in the ultra-distal deposits, and the PDC produced the most voluminous deposits of the eruption.

6.4 The volume, mass and magnitude of the CI

A great part of the pyroclastic current was elutriated or rose into the air as a column during the eruption and dispersed to the east (Thunell et al., 1979; Cornell et al., 1983; Perrotta and Scarpati, 2003; Pyle et al., 2006; Engwell et al., 2014; Scarpati and Perrotta, 2016). The co-ignimbrite phase resulted as a substantial part of the total volume; however, it remains difficult to define the associated absolute volume instead of a percentage of the tephra layer.

The ignimbrite volume (V_i) (4 and 5) without the co-ignimbrite phase can be estimated as follows:

$$\boldsymbol{V_{imin} = V_{pr} + V_m + V_{intr} + 2V_e = 56 + 56 + 16 + 9.6 + 9.6 = 147.2\ km^3} \quad (4)$$

and

$$\boldsymbol{V_{imax} = V_{pr} + V_m + V_{intr} + 2V_e = 67 + 67 + 43.2 + 9.6 + 9.6 = 196.4\ km^3} \quad (5)$$

The total bulk PDC volume obtained by (4) and (5) is 147.2 – 196.4 km^3 (Table 3). The co-ignimbrite volume (V_{ci}) is estimated using the formula (6) based on the crystal concentration method proposed by Scarpati et al., 2014 (3):

$$\boldsymbol{V_{ci} = \frac{Vitric\ loss * V_i}{1 - Vitric\ loss} = \frac{0.65 * V_i}{1 - 0.65} = 273.4 - 364.7\ km^3} \quad (6)$$

The co-ignimbrite volume, using a vitric loss of 0.65, ranges between 273.4 km^3 and 364.7 km^3 (107.6 km^3 – 143.5 km^3 DRE). However, V_{ci} could change a lot, according to the value of vitric loss used. From the literature, Walker (1972) proposed for the outcrop of Altavilla (WGI), near Benevento, a vitric loss of 0.55. Using this data, the co-ignimbrite bulk volume decreases and it is substantially lower between 168.2 km^3 and 240.0 km^3. It is necessary great attention to the right value of vitric loss to use, which can significantly influence the total eruptive volume. In this work, we use 0.65, proposed by Scarpati et al. (2014), which is an average of more samples located in several sites all over the CI distribution and from different units (WGI, LYT and CPF) and it is not quite far from 0.55 previously proposed in literature (Walker, 1972).

The total volume of the material erupted during the PDC phase of the CI eruption ranges between 411 km^3 and 561.1 km^3 (163.2 km^3 – 225.1 km^3 DRE) (Table 3). This estimate is based on the actual preserved deposits of the CI so that all proposed corrections are grounded in a real starting value. Among the previous estimates presented in the literature, the closest to our PDC volume are those proposed by Giaccio (2006) and Pappalardo et al. (2008).

The fallout volume considered in this chapter is the minimum and the maximum proposed in literature by Perrotta and Scarpati (2003) and Marti et al. (2016). However, any of the previous estimates for the fallout volume and any of them could be used in our total volume estimate. The

593 total volume estimate ranges from 415 km^3 to 615.1 km^3 (164.9 km^3 – 247.7 km^3 DRE) (Table 3).
594 These values are similar to some previously proposed total volumes (Cornell et al., 1983; Fedele et
595 al., 2003; Giaccio, 2006; Pyle et al., 2006; Pappalardo et al., 2008; Costa et al., 2012), however, they
596 are constrained, for the fisrt time, to the actual ignimbrite deposit.

597 The mass associated with this volume estimate is (7):

598 $$\boldsymbol{mass_{min} = 164.9\ km^3 * 2608\ kg/m^3 = 4.30 * 10^{14} kg} \quad (7)$$

599 And (8)

600 $$\boldsymbol{mass_{max} = 210.7\ km^3 * 2608\ kg/m^3 = 6.46 * 10^{14} kg} \quad (8)$$

601 and the magnitude (M) (9) (Mason et al., 2004):

602 $$\boldsymbol{M = log10(mass) - 7 = 7.7} \quad (9)$$

603 This value is consistent with a VEI 7 and a M = 7.7, which makes this eruption the largest
604 Quaternary event from the Campi Flegrei caldera and in Europe. Our new volume estimates should
605 help constrain the modeling of the impact on climate and the environment, including on the history of
606 migrations of humans.

607 **7. Conclusions**

608 The CI eruption is the largest eruptive event of the CF caldera and a fundamental chronological
609 marker in all central and eastern Europe. The CI eruption influenced the migration of the hominid
610 groups and it had great effects on the Paleolithic societies (Black et al., 2015; Marti et al., 2016).
611 However, the volume of CI, fundamental to the climate impact and simulations, is poorly
612 constrained. Here we present a review of previous estimations existing in the scientific literature and
613 propose a new method to trace ignimbrite isopachs based on the extrapolation of the paleo-
614 topography that works well in valley-ponded ignimbrites such as the CI, which allows the calculation
615 of well-defined uncertainties on the total volume. A complete isopach map of the ignimbrite is
616 absent, due to the high irregularities of the deposits, feature that this method can overcome. A new
617 entire isopach map of the extracaldera sub-aerial CI pyroclastic flow deposits yields a volume of 61.5
618 km^3 ± 5.5 km^3. The greater part of this volume is in the proximal area (46.4 ± 1.6 km^3, ~75%) while
619 only around the 25% of the volume is in the distal region after the Apennines Mountain (15.1 ± 3.9
620 km^3).

621 Evidence suggests that the same amount of material should be both on land and offshore (e.g. the
622 radial spreading of the flow). The generated submarine currents could have produced a large amount
623 of volcanoclastic deposits in all the submarine canyons in the Gulf of Naples, as in large part of the
624 Tyrrhenian Sea and possibly had a strong impact on the underwater dynamics of that area.
625 Furthermore, the observation of this volcanoclastic layer can help the correlation and the
626 understanding of sediment cores. Including separate estimates of the marine volume, the volume
627 removed by erosion, the intracaldera volume, and the co-ignimbrite ash volume yields a total volume
628 erupted during the PDC phase of 411.0 km^3 to 561.1 km^3 (163.2 km^3 – 225.1 km^3 DRE), these values
629 are in agreement with Giaccio (2006) and Pappalardo et al. (2008), although it is the first time that
630 they are calculated by direct measurements.

A series of error analyses and corrections were applied to reach a total (including Plinian fallout) final volume estimate: 415.0 km^3 – 615.1 km^3 (164.9 km^3 – 247.7 km^3 DRE). The volume of material, ash and aerosols is extremely important to understand and model the climate impact of this eruption, which could affect the intensity of solar radiation and consequently cause short-lived climate changes in a critical period for the modern human as the Middle to Upper Paleolithic transition.

This volume corresponds to a mass of 4.30 - 6.46 x 10^{14} kg, to a magnitude of 7.7 and to a VEI 7. This was a high impact event with significant effect on the climate and populations of the Paleolithic European region and is a proof that the Campi Flegrei caldera was able to generate a devastating eruption of this dimension.

2 Article types

Original Research

3 Manuscript Formatting

3.1 Figure legends

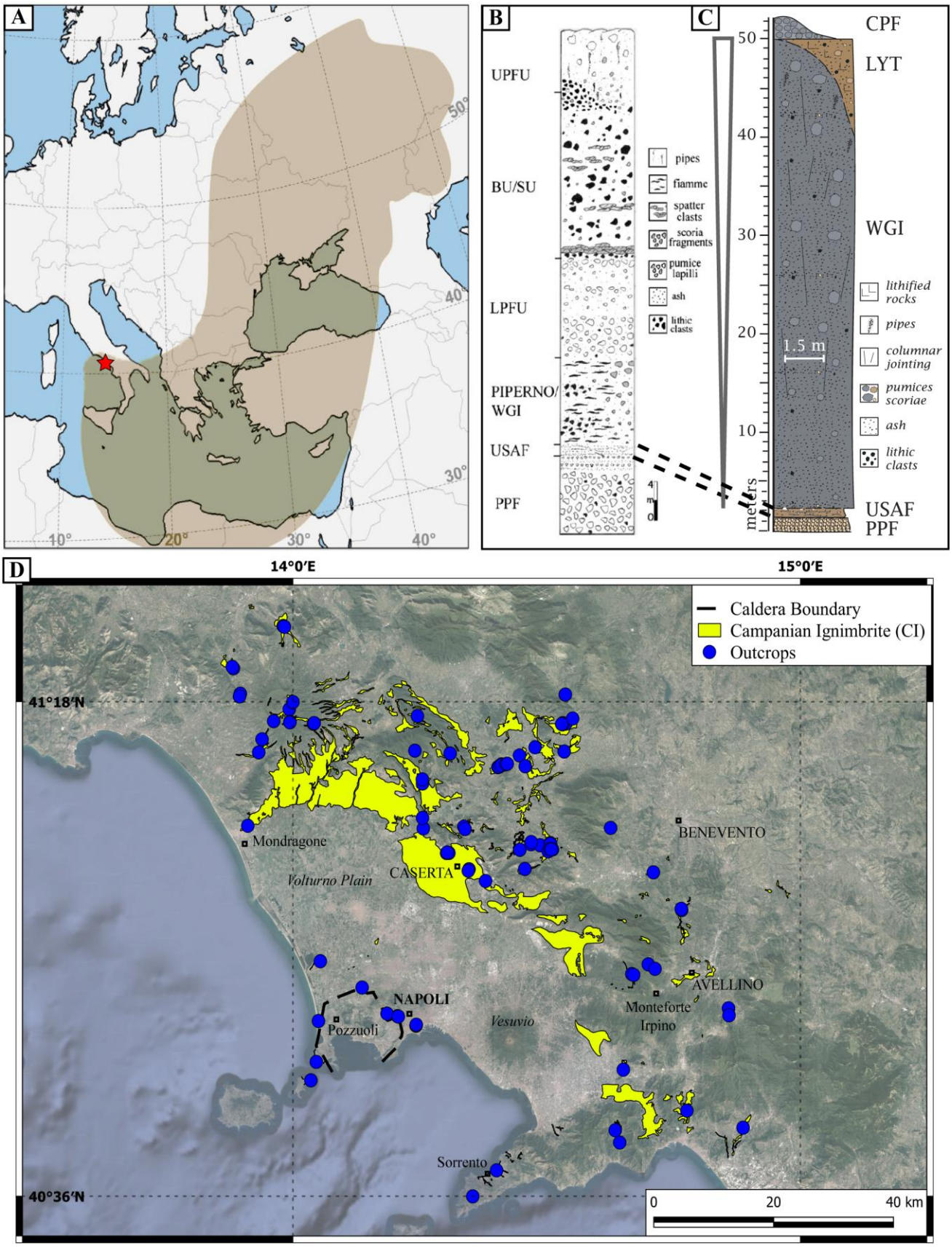
A
10°
20°
30°
40°
50°
40°
30°
B
UPFU
BU/SU
LPFU
PIPERNO/
WGI
USAF
PPF
pipes
fiamme
spatter clasts
scoria fragments
pumice lapilli
ash
lithic clasts
C
CPF
LYT
WGI
USAF
PPF
meters
1.5 m
lithified rocks
pipes
columnar jointing
pumices scoriae
ash
lithic clasts
D
14°0′E
15°0′E
41°18′N
40°36′N
Caldera Boundary
Campanian Ignimbrite (CI)
Outcrops
Mondragone
Volturno Plain
CASERTA
BENEVENTO
AVELLINO
Monteforte
Irpino
NAPOLI
Pozzuoli
Vesuvio
Sorrento
0
20
40 km

645

Figure 1. *The Campanian Ignimbrite distribution.* ***(A)*** *Dispersal area of the CI tephra from the Campi Flegrei caldera (red star), modified from Giaccio et al. (2017). Stratigraphic type-sections of CI proximal (Fedele et al., 2008)* ***(B)*** *and distal* ***(C)*** *deposits.* ***(D)*** *The Campanian Ignimbrite distribution in the Campanian region (the base map is from Google Satellite). Blue dots indicate the location of the studied outcrops (coordinates are reported in the data repository). The maps were generated using the QGIS Open-Source 3.4 (https://www.qgis.org/it/site/).*

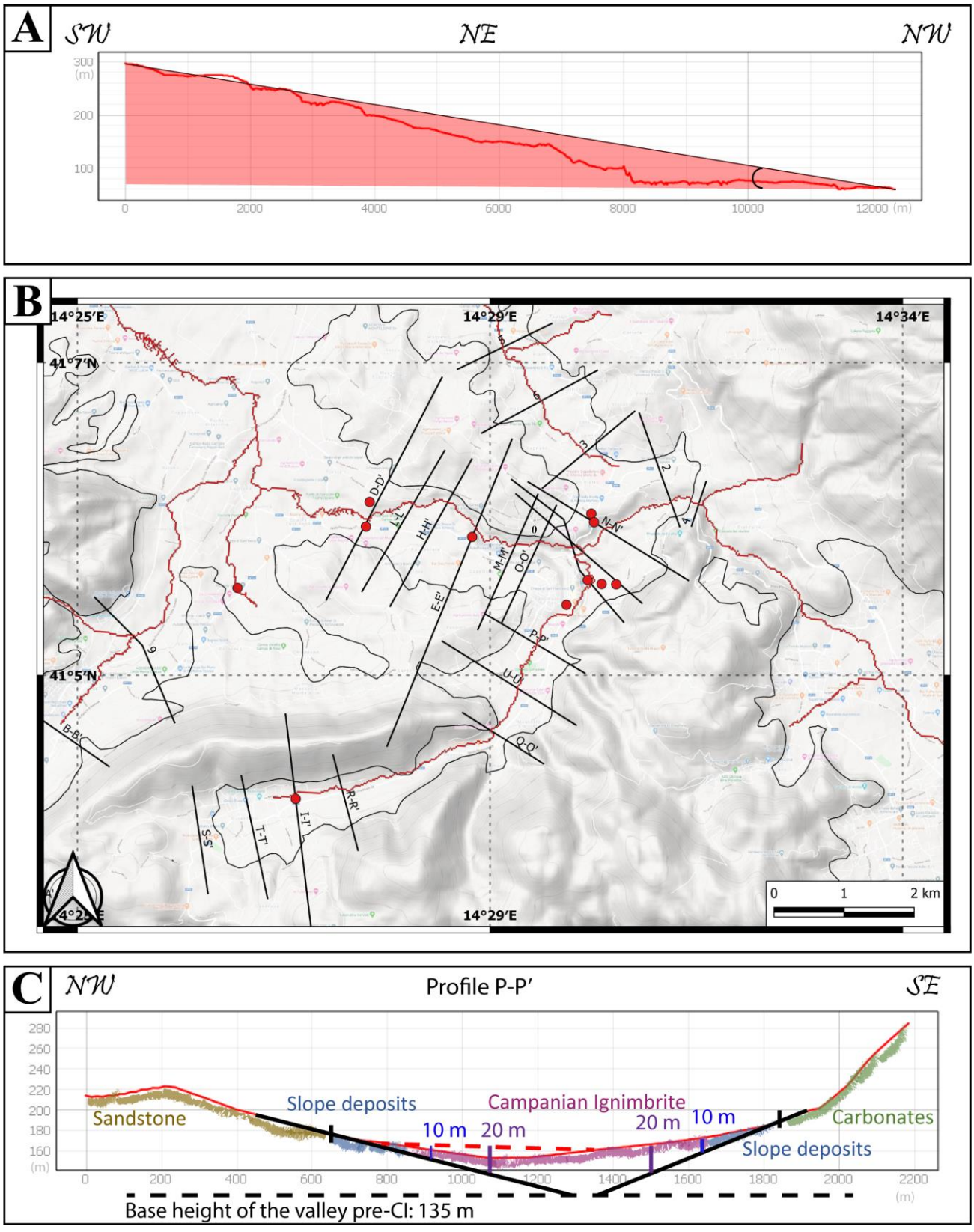

Figure 2. *The topography reconstruction in the Sant'Agata dei Goti area.* ***(A)*** *The modern valley is used as a reference for the paleo-slope during the CI eruption.* ***(B)*** *A series of profiles traced to study the paleo-valley; the red dots are outcrops where the CI is exposed.* ***(C)*** *Reconstruction of the paleo-*

valley in profile P-P', the base elevation is constrained to the CI base observed by fieldwork and to the current slope of the valley. The resulting thickness is always coherent with fieldwork, so where thicknesses are too high, they weren't considered and the isopachs were traced up to a realistic thickness. The numbers represent the thickness of the CI in meters.

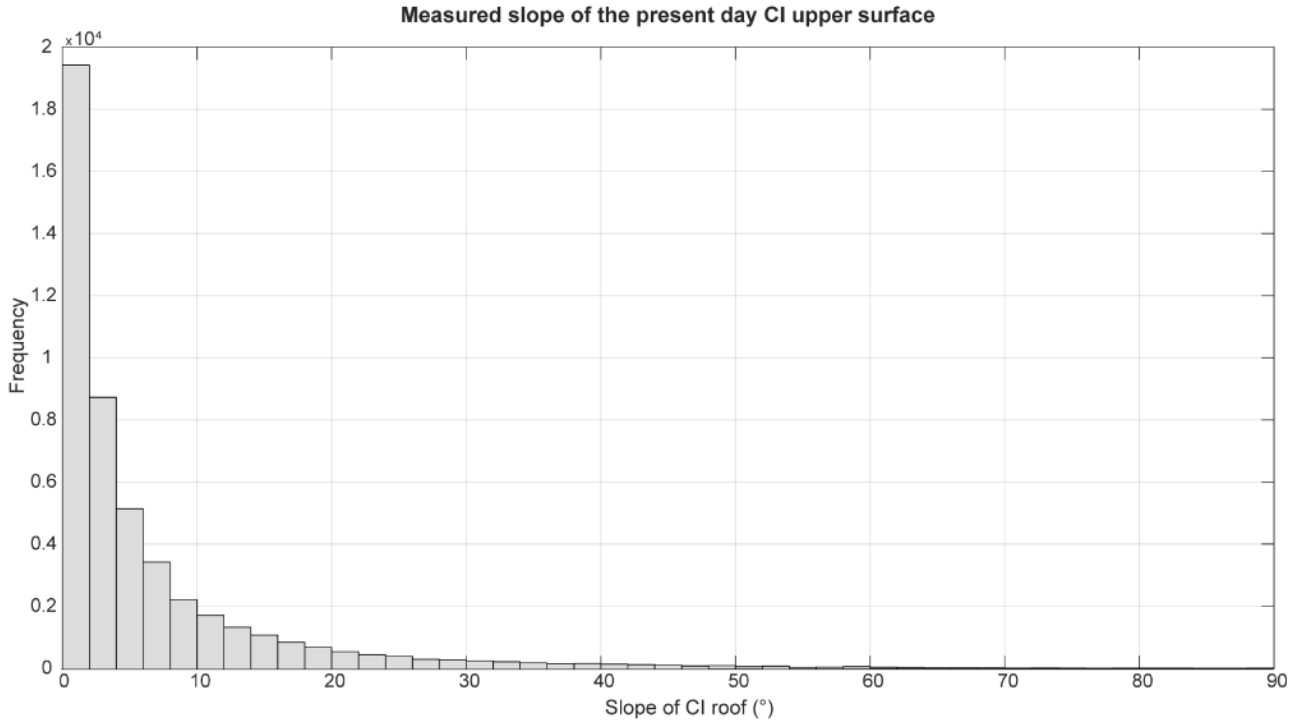

Figure 3. *Frequency of the slope of the upper surface of the CI. At least 80% of the exposed CI upper surface slopes less than 10°.*

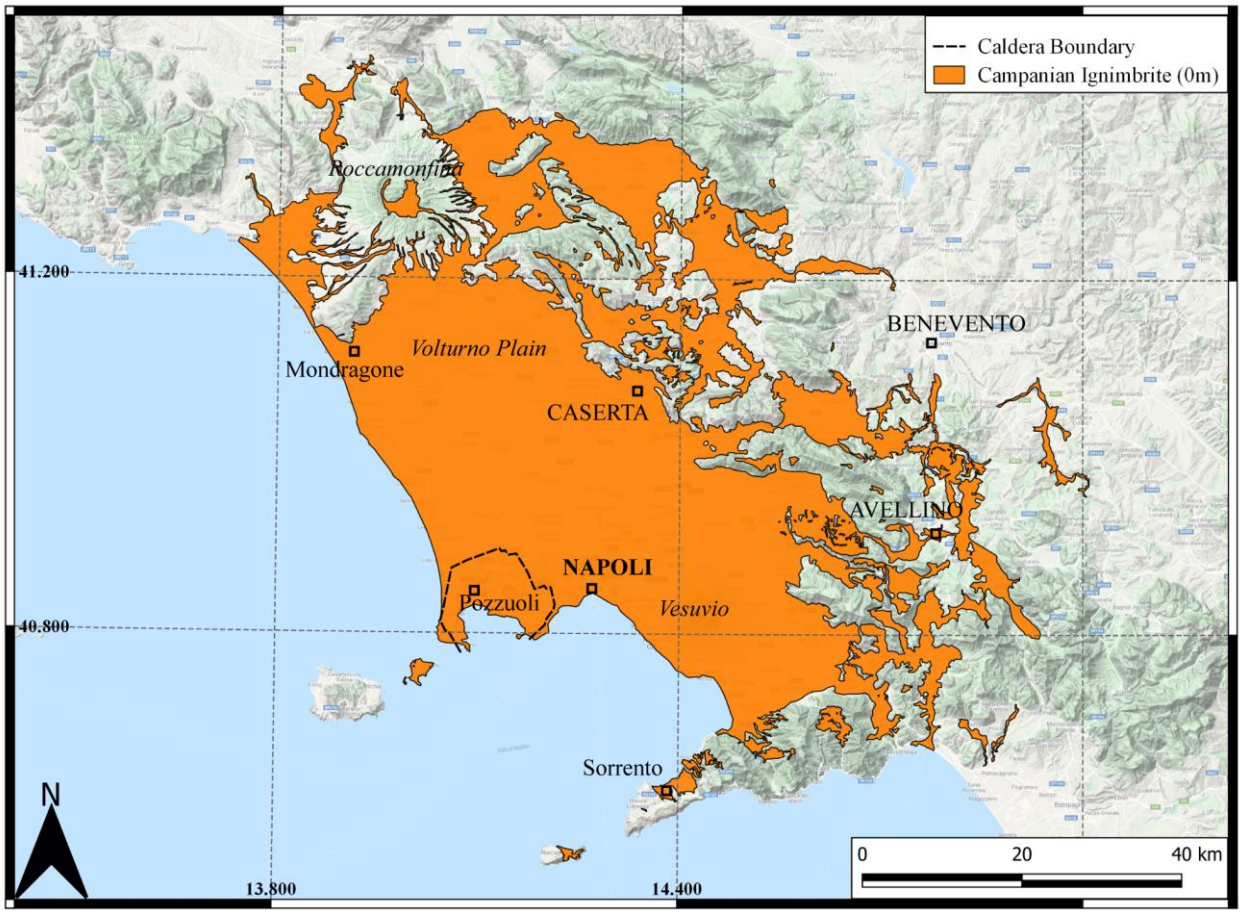

Figure 4. *The areal extent of the CI, enclosed within the isopach 0 m is shown in orange. The total area covered by the preserved deposits of CI is 3216 km^2, the envelopment with a shape is equal to 7547 km^2.*

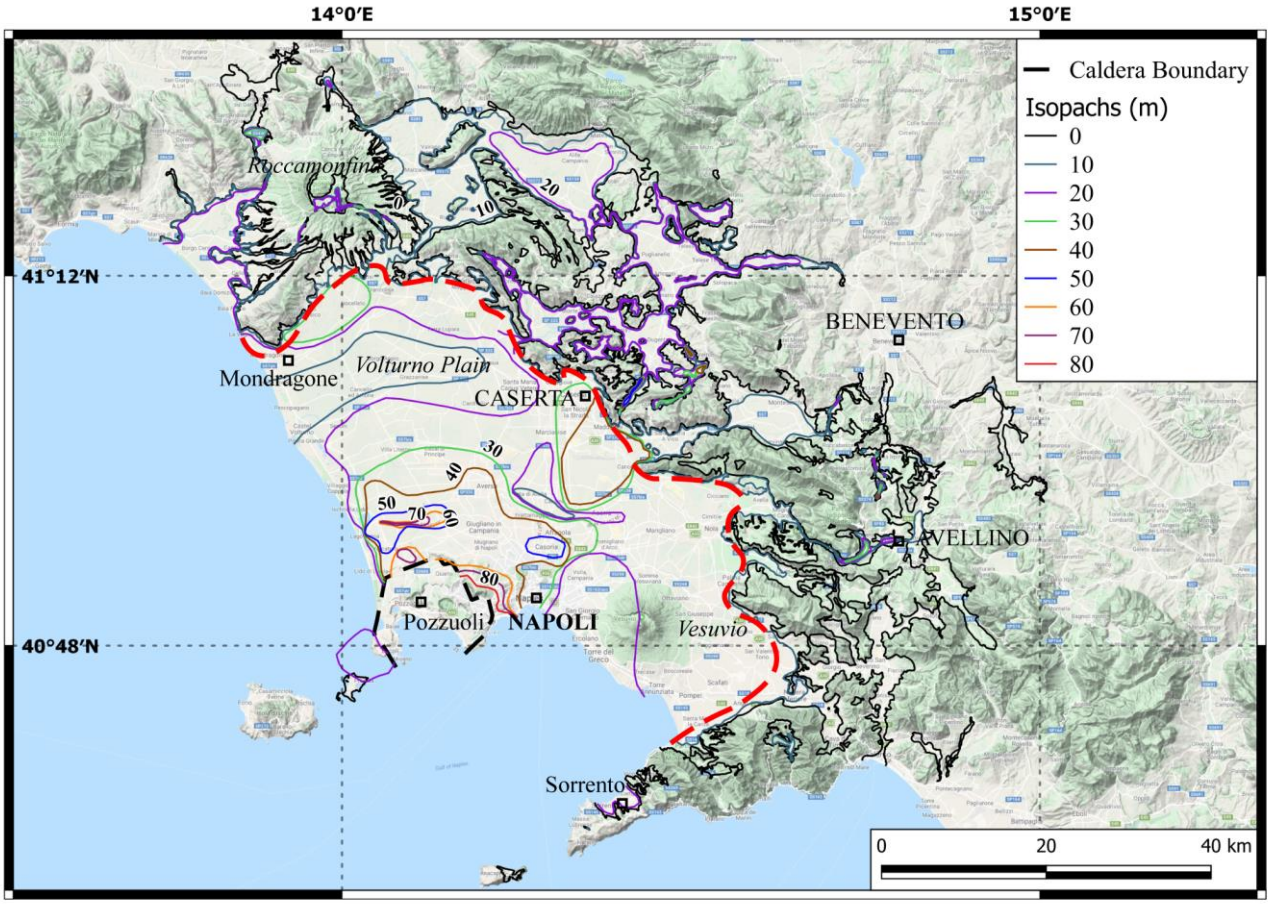

667

668 ***Figure 5.*** *Isopach map of the preserved extra-caldera deposits of the Campanian Ignimbrite. This*
669 *map refers only to the pyroclastic density current deposits; it excludes the Plinian fallout and the co-*
670 *ignimbrite ash. The different colors for each isopach are reported in the map key. The red dashed*
671 *line divides the proximal and the distal area.*

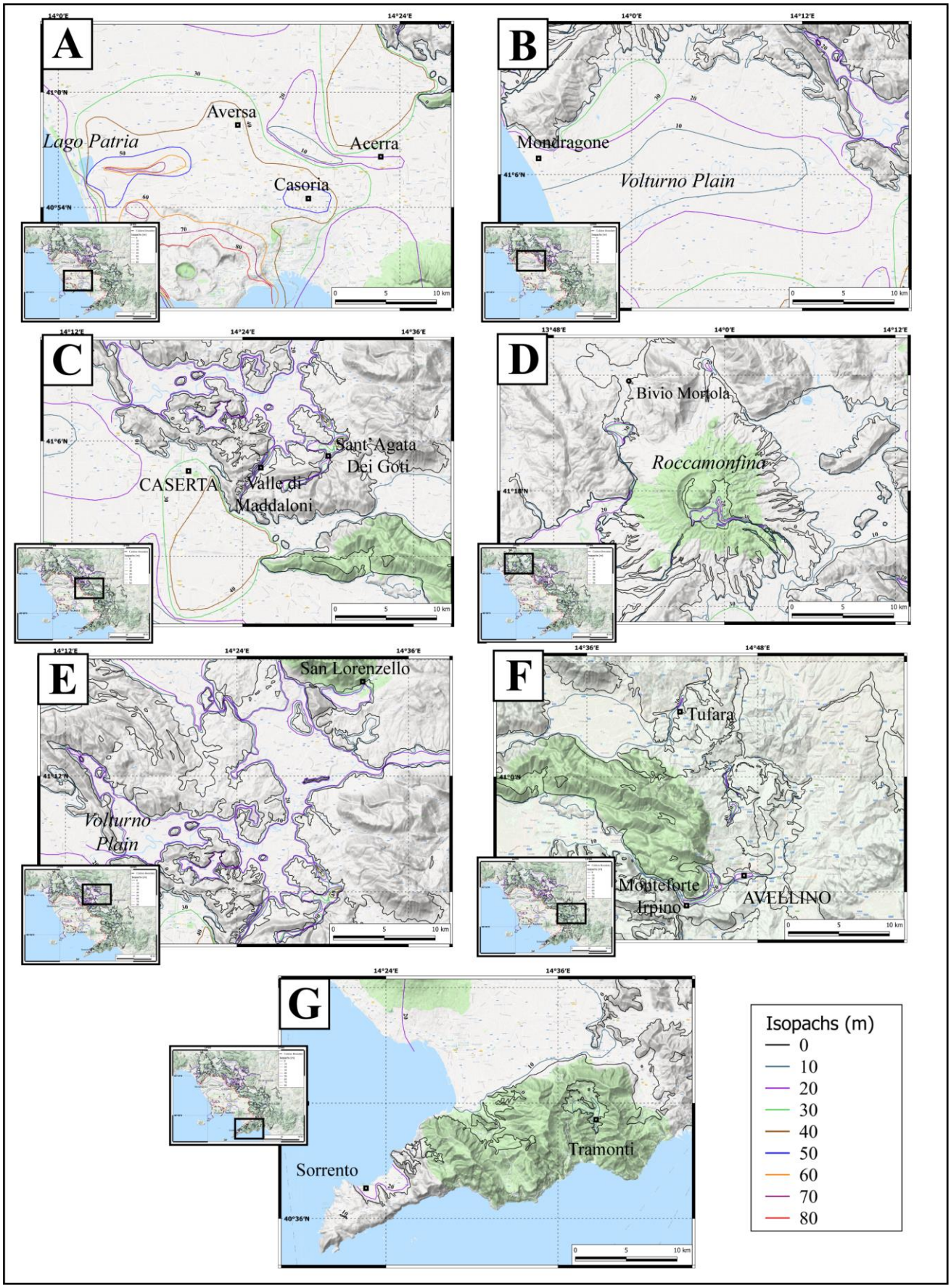
A
Aversa
Lago Patria
Acerra
Casoria
B
Mondragone
Volturno Plain
C
Sant'Agata
Dei Goti
CASERTA
Valle di
Maddaloni
D
Bivio Monola
Roccamonfina
E
San Lorenzello
Volturno
Plain
F
Tufara
Monteforte
Irpino
AVELLINO
G
Tramonti
Sorrento
Isopachs (m)
0
10
20
30
40
50
60
70
80

672

673 ***Figure 6.*** *Detailed isopach maps of selected areas of the Campanian Ignimbrite (excludes fallout):*
674 *(A) north of the caldera, between Lago Patria and Acerra; (B) northern part of the Campanian*
675 *Plain; (C) Apennine ridges east of the Campi Flegrei caldera and the Valley of Maddaloni; (D)*
676 *Roccamonfina and Mortola, in the north of the studied area; (E) Volturno plain and San Lorenzello*
677 *area, northeast of the caldera; (F) distal area of Avellino, southeast of the caldera; (G) Sorrento*
678 *peninsula, in the southern part of the studied area.*

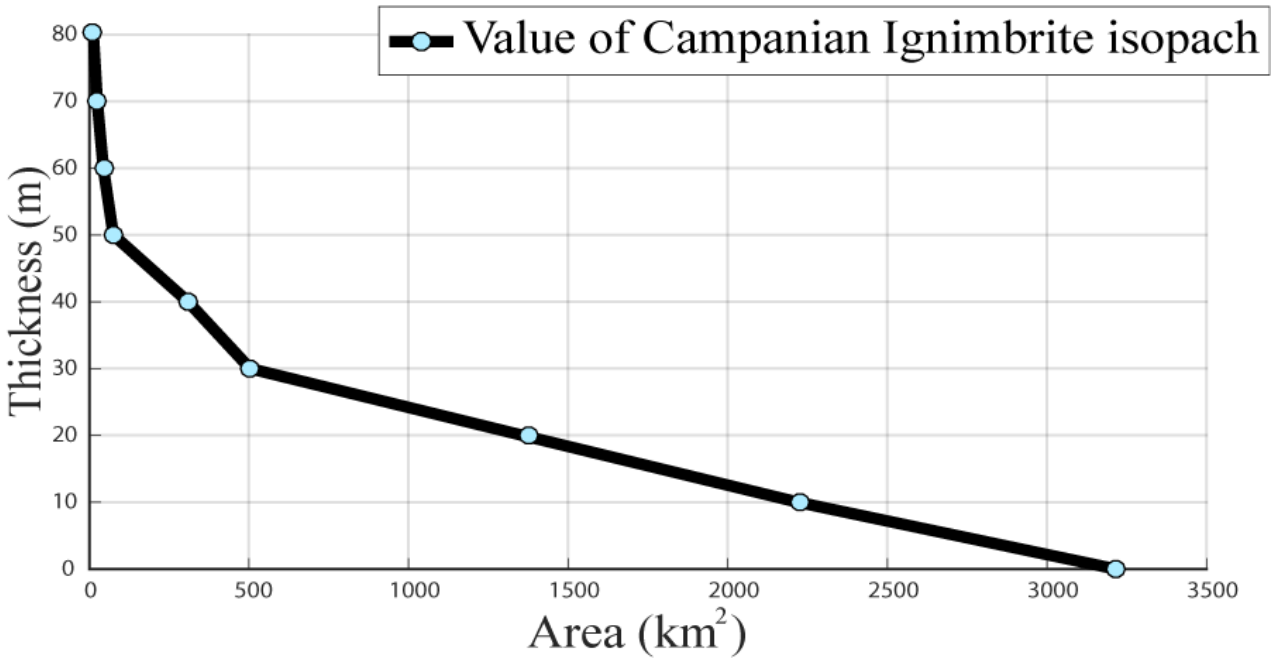

679

680 ***Figure 7.*** *The thickness (m) plotted against the area (km^2) of each isopach of the preserved deposits*
681 *of the CI PDC. The volume is the subtended area of this plot.*

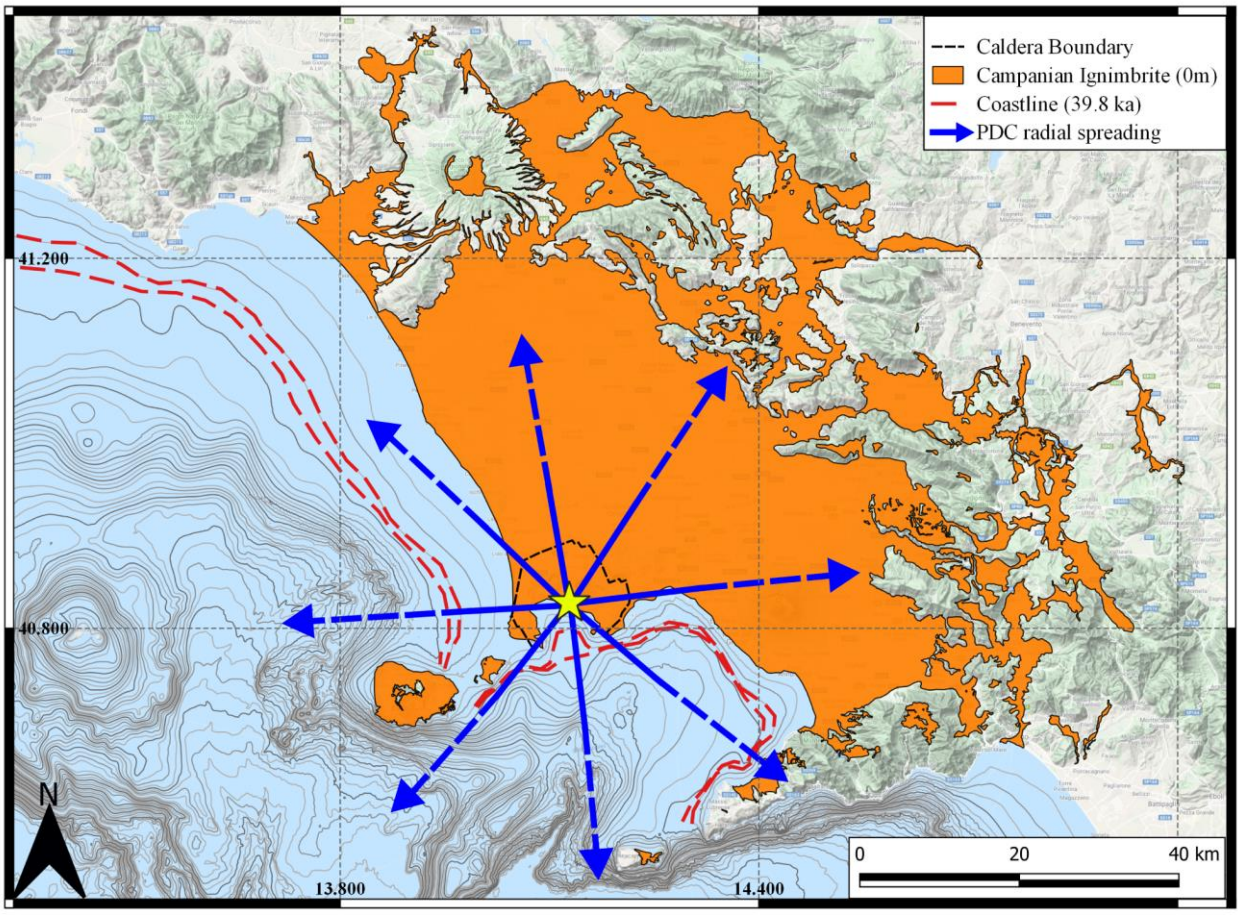

Figure 8. *Bathymetry of the submerged area of the Campi Flegrei Caldera. The red line is the 40 ka coastline, equivalent to -75 – -87 m of the present one. The blue arrows indicate the possible radial spreading of the PDC based on outcrops disposed radially from the center of the Caldera (yellow star) and turbidity currents in the Tyrrhenian Sea. Accumulation of volume south of the caldera is credible, due to the large submarine depressions and valleys.*

3.2 Tables

	Volume calculations (km^3)					
Authors	Plinian fallout	Co-plinian ash	PDC	Co-ignimbrite ash	Y-5	Total
Thunell et al., 1979			30-40*		30-40*	60-80*
Cornell et al., 1983					73	>150
Fisher et al., 1993			500			
Civetta et al., 1997	25*		120*			145*
Rosi et al., 1999	15					
Fedele et al., 2003						200*

Perrotta and Scarpati, 2003	4	16		100 (42*)		
Rolandi et al., 2003			180	140		320 (200*)
Giaccio, 2006	10 (3*)		385 (215*)	180 (86*)		575 (300*)
Marianelli et al., 2006	20*		130*			150*
Pyle et al., 2006				72-120 (31-50*)		105-210*
Pappalardo et al., 2008	20*		180*			200*
Costa et al., 2012					250-300 (104-125*)	430-680 (180-280*)
Scarpati et al., 2014			54 (25*)	100 (42*)		
Marti et al., 2016	54 (22.6*)			153.9 (61.6*)		207.9 (84.2*)
Scarpati and Perrotta, 2016	5.33 (0.88*)	14.67 (6.88*)				

Table 1. *Bulk and DRE (*) volume calculations proposed for the CI by different authors, in approximate chronological order. Y-5 refers to those studies that did not identify the co-plinian and co-ignimbrite contribution. The methods are described in the text.*

Thickness (km)	**Area (m^2)**	**Area (km^2)**	**Cumulative area (km^2)**	**Volume (km^3)**	**Cumulative Volume (km^3)**	**Volume (%)**
0.08	12613584.05	12.61	12.61	0.19	0.19	0.33
0.07	12329142.98	12.33	24.94	0.16	0.35	0.28
0.06	19116655.52	19.12	44.06	0.25	0.60	0.44
0.05	31312007.72	31.31	75.37	1.33	1.92	2.34
0.04	234023868.7	234.02	309.40	2.14	4.07	3.78
0.03	194514229.9	194.51	503.91	5.24	9.31	9.24
0.02	853977772.9	853.98	1357.89	8.58	17.89	15.13
0.01	862025846	862.03	2219.91	9.29	27.18	16.38
0-0.009		995.70	3215.61	34.32	**61.50**	60.52

Table 2. *The values of thickness (m), area (km^2), volume (km^3), cumulative volume (km^3) and the percentage of volume for each isopach.*

	Bulk Volume (km^3)	**DRE Volume (km^3)**
Preserved extra-caldera ignimbrite volume	56 – 67	22.0 – 26.4

Marine volume	56 – 67	22.0 – 26.4
Intracaldera volume	16 – 43.2	7.9 – 21.4
Areal erosion	9.6	3.7
Co-ignimbrite ash volume	273.4 – 364.7	107.6 – 143.5
Total PDC volume	411 – 561.1	163.2 – 225.1
Fallout volume (Perrotta and Scarpati, 2003; Marti et al., 2016)	4 – 54	1.7 – 22.6
Total CI volume	415 – 615.1	164.9 – 247.7

Table 3. *The volume of the CI eruption. The various parts of the PDC volume estimate are explained in the text. The fallout volume considered in this work is the maximum and the minimum proposed in literature by Perrotta and Scarpati (2003) and Marti et al. (2016).*

4 Nomenclature

Abbreviations and acronyms

a.s.l.: above sea level; BU: Breccia Unit; CCDB: Collapse Caldera Database; CE: Common Era; CF: Campi Flegrei; CI: Campanian Ignimbrite; CPF: Coarse Pumice Flow; DEM: Digital Elevation Model; DRE: Dense Rock Equivalent; ka: Thousands of years ago; LAMEVE: Large Magnitude Explosive Volcanic Eruptions; LPFU: Lower Pumice Flow Unit; LYT: Lithified Yellow Tuff; M: Magnitude; NYT: Neapolitan Yellow Tuff; PDC: Pyroclastic Density Current; PPF: Plinian Pumice Fallout; SU: Spatter Unit; UPFU: Upper Pumice Flow Unit; USAF: Unconsolidated Stratified Ash Flow; V: total volume; V_{ci}: co-ignimbrite ash fall volume; V_{cpf}: co-plinian fall volume; V_e: areal erosion volume; VEI: Volcanic Explosivity Index; V_g: geometric volume; V_i: ignimbrite volume; V_{intr}: intracaldera volume; V_m: marine volume; V_{mx}: matrix volume; V_{pdc}: pyroclastic density current volume; V_{pf}: mass ejected during the phases that produced Plinian columns; V_{ppf}: plinian fallout volume; V_{pr}: preserved extra-caldera bulk volume; WGI: Welded Gray Ignimbrite; ρ: bulk density; φ_t: total porosity.

5 Conflict of Interest

The authors declare that the research was conducted in the absence of any commercial or financial relationships that could be construed as a potential conflict of interest.

6 Author Contributions

AS conducted field work, analysis, wrote the draft of this manuscript and made the figures. GG designed the research and helped in the development of the method. RI contributed to data collection. All the authors contributed to the field work, reviewed and edited the draft.

7 Funding

AS and GG gratefully acknowledge The Grant of Excellence Departments, MIUR-Italy. Partial support for some field costs was provided by NSF EAR1761713 to MHO.

8 Acknowledgments

AS and GG gratefully acknowledge The Grant of Excellence Departments, MIUR-Italy. AS thanks Emanuele Sciarrino and Rose Gallo for their help in the fieldwork. We thank Danilo M. Palladino for discussions. Partial support for some field costs was provided by NSF EAR1761713 to MHO.

9 References

Acocella, V. (2008). Activating and reactivating pairs of nested collapses during caldera-forming eruptions: Campi Flegrei (Italy). *Geophys. Res. Lett.* 35, 1–5. doi:10.1029/2008GL035078.

Albert, P. G., Giaccio, B., Isaia, R., Costa, A., Niespolo, E. M., Nomade, S., et al. (2019). Evidence for a large-magnitude eruption from Campi Flegrei caldera (Italy) at 29 ka. *Geology* 47, 595–599. doi:10.1130/G45805.1.

Aldiss, D. T., and Ghazali, S. A. (1984). The regional geology and evolution of the Toba volcano-tectonic depression, Indonesia. *J. Geol. Soc. London.* 141, 487–500. doi:10.1144/gsjgs.141.3.0487.

Allen, S. R., and Cas, R. A. F. (2001). Transport of pyroclastic flows across the sea during the explosive, rhyolitic eruption of the Kos Plateau Tuff, Greece. *Bull. Volcanol.* 62, 441–456. doi:10.1007/s004450000107.

Anikovich, M., Sinitsyn, A. A., Hoffecker, J. F., Holliday, V. T., Popov, V. V., Lisitsyn, S. N., et al. (2007). Early Upper Paleolithic in Eastern Europe and Implications for the Dispersal of Modern Humans. *Science (80-.).* 315, 223–226. doi:10.1126/science.1133376.

Antonioli, F. (2012). Sea level change in Western-Central Mediterranean since 300 kyr: Comparing global sea level curves with observed data. *Alp. Mediterr. Quat.* 25, 15–23.

Antonioli, F., Bard, E., Potter, E. K., Silenzi, S., and Improta, S. (2004). 215-ka history of sea-level oscillations from marine and continental layers in Argentarola Cave speleothems (Italy). *Glob. Planet. Change* 43, 57–78. doi:10.1016/j.gloplacha.2004.02.004.

Barberi, F., Innocenti, F., Lirer, L., Munno, R., Pescatore, T., and Santacroce, R. (1978). The campanian ignimbrite: a major prehistoric eruption in the Neapolitan area (Italy). *Bull. Volcanol.* 41, 10–31. doi:10.1007/BF02597680.

Barsotti, S., Neri, A., and Scire, J. S. (2008). The VOL-CALPUFF model for atmospheric ash dispersal: 1. Approach and physical formulation. *J. Geophys. Res. Solid Earth* 113, 1–12. doi:10.1029/2006JB004623.

Bellucci, F. (1994). Nuove conoscenze stratigrafiche sui depositi vulcanici del sottosuolo del settore meridionale della piana campana. *Boll. Soc. Geol. It.* 113, 395–420.

Best, M. G., Christiansen, E. H., Deino, A. L., Gromme, S., Hart, G. L., and Tingey, D. G. (2013a). The 36-18 Ma Indian Peak-Caliente ignimbrite field and calderas, southeastern Great Basin,

755 USA: Multicyclic super-eruptions. *Geosphere* 9, 864–950. doi:10.1130/GES00902.1.

756 Best, M. G., Gromme, S., Deino, A. L., Christiansen, E. H., Hart, G. L., and Tingey, D. G. (2013b).
757 The 36-18 ma central nevada ignimbrite field and calderas, Great basin, USA: Multicyclic
758 super-eruptions. *Geosphere* 9, 1562–1636. doi:10.1130/GES00945.1.

759 Black, B. A., Neely, R. R., and Manga, M. (2015). Campanian Ignimbrite volcanism, climate, and the
760 final decline of the Neanderthals. *Geology* 43, 411–414. doi:10.1130/G36514.1.

761 Bluszcz, A., Hercman, H., Pazdur, A., and Pazdur, M. (1992). "Radiometric dating," in *Temnata*
762 *Cave. Excavations in Karlukovo Karst Area, Bulgaria vol. 1.1*, eds. J. K. Kozlowski, H. Laville,
763 and B. Ginter (Cracow: Jagellonian University Press), 223–240.

764 Bonadonna, C., Connor, C. B., Houghton, B. F., Connor, L., Byrne, M., Laing, A., et al. (2005).
765 Probabilistic modeling of tephra dispersal: Hazard assessment of a multiphase rhyolitic eruption
766 at Tarawera, New Zealand. *J. Geophys. Res. Solid Earth* 110, 1–21. doi:10.1029/2003JB002896.

767 Bonadonna, C., Ernst, G. G. J., and Sparks, R. S. J. (1998). Thickness variations and volume
768 estimates of tephra fall deposits: the importance of particle Reynolds number. *J. Volcanol.*
769 *Geotherm. Res.* 81, 173–187. doi:10.1016/S0377-0273(98)00007-9.

770 Bonadonna, C., and Phillips, J. C. (2003). Sedimentation from strong volcanic plumes. *J. Geophys.*
771 *Res. Solid Earth* 108, 1–28. doi:10.1029/2002jb002034.

772 Brown, R. J., and Andrews, G. D. M. (2015). "Deposits of pyroclastic density currents," in *The*
773 *Encyclopedia of Volcanoes*, 631–648.

774 Calanchi, N., Cattaneo, A., Dinelli, E., Gasparotto, G., and Lucchini, F. (1998). Tephra layers in Late
775 Quaternary sediments of the central Adriatic Sea. *Mar. Geol.* 149, 191–209. doi:10.1016/S0025-
776 3227(98)00030-9.

777 Capocci, E. (1835). Nuove ricerche sul noto fenomeno delle colonne perforate dalle Foladi nel
778 tempio di Serapide in Pozzuoli.

779 Cappelletti, P., Cerri, G., Colella, A., de'Gennaro, M., Langella, A., Perrotta, A., et al. (2003). Post-
780 eruptive processes in the Campanian Ignimbrite. *Mineral. Petrol.* 79, 79–97.
781 doi:10.1007/s00710-003-0003-7.

782 Carey, S., Sigurdsson, H., Mandeville, C., and Bronto, S. (1996). Pyroclastic flows and surges over
783 water: an example from the 1883 Krakatau eruption. *Bull. Volcanol.* 57, 493–511.
784 doi:10.1007/BF00304435.

785 Cashman, K. V., and Giordano, G. (2014). Calderas and magma reservoirs. *J. Volcanol. Geotherm.*
786 *Res.* 288, 28–45. doi:10.1016/j.jvolgeores.2014.09.007.

787 Castagnoli, G. C., Albrecht, A., Beer, J., Shen, C., Callegari, E., Taricco, C., et al. (1995). Evidence
788 for enhanced 10Be deposition in Mediterranean sediments 35 Kyr BP. *Geophys. Res. Lett.* 22,
789 707–710.

790 Civetta, L., Orsi, G., Pappalardo, L., Fisher, R. V., Heiken, G., and Ort, M. H. (1997). Geochemical

zoning, mingling, eruptive dynamics and depositional processes - the Campanian Ignimbrite, Campi Flegrei caldera, Italy. *J. Volcanol. Geotherm. Res.* 75, 183–219.

Cornell, W., Carey, S., and Sigurdsson, H. (1983). Computer simulation of transport and deposition of the campanian Y-5 ash. *J. Volcanol. Geotherm. Res.* 17, 89–109. doi:10.1016/0377-0273(83)90063-X.

Costa, A., Folch, A., Macedonio, G., Giaccio, B., Isaia, R., and Smith, V. C. (2012). Quantifying volcanic ash dispersal and impact of the Campanian Ignimbrite super-eruption. *Geophys. Res. Lett.* 39, 3–7. doi:10.1029/2012GL051605.

Costa, A., Macedonio, G., and Folch, A. (2006). A three-dimensional Eulerian model for transport and deposition of volcanic ashes. *Earth Planet. Sci. Lett.* 241, 634–647. doi:10.1016/j.epsl.2005.11.019.

Costa, A., Suzuki, Y. J., and Koyaguchi, T. (2018). Understanding the plume dynamics of explosive super-eruptions. *Nat. Commun.* 9. doi:10.1038/s41467-018-02901-0.

Cramp, A., Vitaliano, C. J., and Collins, M. B. (1989). Identification and dispersion of the campanian ash layer (Y-5) in the sediments of the Eastern Mediterranean. *Geo-Marine Lett.* 9, 19–25. doi:10.1007/BF02262814.

Crosweller, H. S., Brown, S. K., Deligne, N. I., Guerrero, N. O., Hobbs, L., Sparks, R. S. J., et al. (2012). Global database on large magnitude explosive volcanic eruptions (LaMEVE). *J. Appl. Volcanol.* 1, 1–13. doi:10.1186/2191-5040-1-4.

D'Oriano, C., Poggianti, E., Bertagnini, A., Cioni, R., Landi, P., Polacci, M., et al. (2005). Changes in eruptive style during the A.D. 1538 Monte Nuovo eruption (Phlegrean Fields, Italy): The role of syn-eruptive crystallization. *Bull. Volcanol.* 67, 601–621. doi:10.1007/s00445-004-0397-z.

De Natale, G., Troise, C., Mark, D., Mormone, A., Piochi, M., Di Vito, M. A., et al. (2016). The Campi Flegrei Deep Drilling Project (CFDDP): New insight on caldera structure, evolution and hazard implications for the Naples area (Southern Italy). *Geochemistry Geophys. Geosystems* 17, 2825–2834. doi:10.1002/2016GC006406.

De Vivo, B., Rolandi, G., Gans, P. B., Calvert, A., Bohrson, W. A., Spera, F. J., et al. (2001). New constraints on the pyroclastic eruptive history of the Campanian volcanic Plain (Italy). *Mineral. Petrol.* 73, 47–65. doi:10.1007/s007100170010.

Di Vito, M. A., Isaia, R., Orsi, G., Southon, J., De Vita, S., D'Antonio, M., et al. (1999). Volcanism and deformation since 12,000 years at the Campi Flegrei caldera (Italy). *J. Volcanol. Geotherm. Res.* 91, 221–246. doi:10.1016/S0377-0273(99)00037-2.

Dufek, J., and Bergantz, G. W. (2007). Dynamics and deposits generated by the Kos Plateau Tuff eruption: Controls of basal particle loss on pyroclastic flow transport. *Geochemistry, Geophys. Geosystems* 8. doi:10.1029/2007GC001741.

Dufek, J., Manga, M., and Staedter, M. (2007). Littoral blasts: Pumice-water heat transfer and the conditions for steam explosions when pyroclastic flows enter the ocean. *J. Geophys. Res. Solid Earth* 112, 1–16. doi:10.1029/2006JB004910.

Engwell, S., Sparks, R. S. J., and Carey, S. (2014). Physical characteristics of tephra layers in the deep sea realm: the Campanian Ignimbrite eruption. *Geol. Soc. London, Spec. Publ.* 398, 47–64. doi:10.1144/SP398.7.

Fedele, F. G., Giaccio, B., and Hajdas, I. (2008a). Timescales and cultural process at 40,000 BP in the light of the Campanian Ignimbrite eruption, Western Eurasia. *J. Hum. Evol.* 55, 834–857. doi:10.1016/j.jhevol.2008.08.012.

Fedele, F. G., Giaccio, B., Isaia, R., and Orsi, G. (2002). Ecosystem Impact of the Campanian Ignimbrite Eruption in Late Pleistocene Europe. *Quat. Res.* 57, 420–424. doi:10.1006/qres.2002.2331.

Fedele, F. G., Giaccio, B., Isaia, R., and Orsi, G. (2003). The Campanian ignimbrite eruption, Heinrich event 4, and Palaeolithic change in Europe: a high-resolution investigation. *Geophys. Monogr.*, 301–325. doi:10.1029/139GM20.

Fedele, F. G., Giaccio, B., Isaia, R., Orsi, G., Carroll, M. R., and Scaillet, B. (2007). The Campanian Ignimbrite Factor: Towards a Reappraisal of the Middle to Upper Palaeolithic "Transition." *Living Under Shad. Cult. Impacts Volcan. Eruptions*, 19–41.

Fedele, L., Scarpati, C., Lanphere, M., Melluso, L., Morra, V., Perrotta, A., et al. (2008b). The Breccia Museo formation, Campi Flegrei, southern Italy: Geochronology, chemostratigraphy and relationship with the Campanian Ignimbrite eruption. *Bull. Volcanol.* 70, 1189–1219. doi:10.1007/s00445-008-0197-y.

Fedele, L., Scarpati, C., Sparice, D., Perrotta, A., and Laiena, F. (2016). A chemostratigraphic study of the Campanian Ignimbrite eruption (Campi Flegrei, Italy): Insights on magma chamber withdrawal and deposit accumulation as revealed by compositionally zoned stratigraphic and facies framework. *J. Volcanol. Geotherm. Res.* 324, 105–117. doi:10.1016/j.jvolgeores.2016.05.019.

Fierstein, J., and Hildreth, W. (1992). The plinian eruptions of 1912 at Novarupta, Katmai National Park, Alaska. *Bull. Volcanol.* 54, 646–684. doi:10.1007/BF00430778.

Fisher, R. V., Orsi, G., Ort, M. H., and Heiken, G. (1993). Mobility of a large-volume pyroclastic flow - emplacement of the Campanian ignimbrite, Italy. *J. Volcanol. Geotherm. Res.* 56, 205–220. doi:10.1016/0377-0273(93)90017-L.

Folch, A. (2012). A review of tephra transport and dispersal models: Evolution, current status, and future perspectives. *J. Volcanol. Geotherm. Res.* 235–236, 96–115. doi:10.1016/j.jvolgeores.2012.05.020.

Folch, A., Costa, A., Durant, A., and Macedonio, G. (2010). A model for wet aggregation of ash particles in volcanic plumes and clouds: 2. Model application. *J. Geophys. Res. Solid Earth* 115, 1–16. doi:10.1029/2009JB007176.

Folkes, C. B., Wright, H. M. N., Cas, R. A. F., de Silva, S. L., Lesti, C., and Viramonte, J. G. (2011). A re-appraisal of the stratigraphy and volcanology of the Cerro Galán volcanic system, NW Argentina. *Bull. Volcanol.* 73, 1427–1454. doi:10.1007/s00445-011-0459-y.

867 Geyer, A., and Martí, J. (2008). The new worldwide collapse caldera database (CCDB): A tool for
868 studying and understanding caldera processes. *J. Volcanol. Geotherm. Res.* 175, 334–354.
869 doi:10.1016/j.jvolgeores.2008.03.017.

870 Giaccio, B. (2006). L'eruzione dell'Ignimbrite Campana (c . 40 ka BP), oscillazioni climatiche sub-
871 orbitali e i cambiamenti bioculturali dell'OIS 3 europeo.

872 Giaccio, B., Hajdas, I., Isaia, R., Deino, A. L., and Nomade, S. (2017). dating of the Campanian
873 Ignimbrite (Y-5) reconciles the time-scales of climatic-cultural processes at 40 ka. *Nat. Publ.*
874 *Gr.*, 1–10. doi:10.1038/srep45940.

875 Giaccio, B., Hajdas, I., Peresani, M., Fedele, F. G., and Isaia, R. (2006). "The Campanian Ignimbrite
876 tephra and its relevnce for the timing of the middle to upper paleolithic shift," in *When*
877 *Neanderthals and modern humans met*, 343–375.

878 Giaccio, B., Isaia, R., Fedele, F. G., Di Canzio, E., Hoffecker, J. F., Ronchitelli, A., et al. (2008). The
879 Campanian Ignimbrite and Codola tephra layers: Two temporal/stratigraphic markers for the
880 Early Upper Palaeolithic in southern Italy and eastern Europe. *J. Volcanol. Geotherm. Res.* 177,
881 208–226. doi:10.1016/j.jvolgeores.2007.10.007.

882 Giordano, G., and Doronzo, D. M. (2017). Sedimentation and mobility of PDCs: a reappraisal of
883 ignimbrites' aspect ratio. *Sci. Rep.* 7, 4444. doi:10.1038/s41598-017-04880-6.

884 Hajdas, I., Taricco, C., Bonani, G., Beer, J., Bernasconi, S. M., and Wacker, L. (2011). Anomalous
885 radiocarbon ages found in Campanian Ignimbrite deposit of the Mediterranean deep-sea core
886 CT85-5. *Radiocarbon* 53, 575–583.

887 Harkovska, A. V., Zlatkova, M. J., Chochov, S. D., and Vergilova, Z. I. (1990). "Campanian area
888 tephra on the territory of Bulgaria," in *IAVCEI International Volcanological Congress*, Vo. 3,
889 No. 8.

890 Henry, C. D., and Price, J. G. (1984). Variations in caldera development in the Tertiary volcanic field
891 of Trans-Pecos Texas. *J. Geophys. Res.* 89, 8765–8786. doi:10.1029/JB089iB10p08765.

892 Isaia, R., Marianelli, P., and Sbrana, A. (2009). Caldera unrest prior to intense volcanism in Campi
893 Flegrei (Italy) at 4.0 ka B.P.: Implications for caldera dynamics and future eruptive scenarios.
894 *Geophys. Res. Lett.* 36, 1–6. doi:10.1029/2009GL040513.

895 ISPRA (2009). Geological Map n. 432 ''Benevento''; scale 1:50,000. National Geological Survey of
896 Italy, Università degli studi di Urbino, Istituto di Geologia Applicata, Urbino, Italy.

897 ISPRA (2010). Geological Map n. 431 ''Caserta Est''; scale 1:50,000. National Geological Survey of
898 Italy, Regione Campania, Settore Difesa Suolo, Napoli, Italy.

899 ISPRA (2011a). Geological Map n. 465 ''Isola di Procida''; scale 1:50,000. National Geological
900 Survey of Italy, Regione Campania, Settore Difesa Suolo, Napoli, Italy.

901 ISPRA (2011b). Geological Map n. 448 ''Ercolano''; scale 1:50,000. National Geological Survey of
902 Italy, CNR Consiglio Nazionale delle Ricerche, Italy.

ISPRA (2011c). Geological Map n. 467 ‘‘Salerno’’; scale 1:50,000. National Geological Survey of Italy, (http://www.isprambiente.gov.it/MEDIA/carg/ campania.html).

ISPRA (2011d). Geological Map n. 446-447 ‘‘Napoli’’; scale 1:50,000. National Geological Survey of Italy, Regione Campania - Settore Difesa Suolo, Napoli, Italy.

ISPRA (2014a). Geological Map n. 450 ‘‘S.Angelo dei Lombardi’’; scale 1:50,000. National Geological Survey of Italy, CNR Consiglio Nazionale delle Ricerche, Italy.

ISPRA (2014b). Geological Map n. 466-485 ‘‘Sorrento-Termini’’; scale 1:50,000. National Geological Survey of Italy, CNR Consiglio Nazionale delle Ricerche, Italy.

ISPRA (2016). Geological Map n. 449 ‘‘Avellino’’; scale 1:50,000. National Geological Survey of Italy, Regione Campania, Italy.

ISPRA (2018). Geological Map n. 464 ‘‘Isola d’Ischia’’; scale 1:25,000. National Geological Survey of Italy, Regione Campania, Settore Difesa Suolo, Napoli, Italy.

Keller, J., Ryan, W. B. F., Ninkovich, D., and Altherr, R. (1978). Explosive volcanic activity in the Mediterranean over the past 200,000 yr as recorded in deep-sea sediments. *Bull. Geol. Soc. Am.* 89, 591–604. doi:10.1130/0016-7606(1978)89<591:EVAITM>2.0.CO;2.

Knight, M. D., Walker, G. P. L., Ellwood, B. B., and Diehl, J. F. (1986). Stratigraphy, paleomagnetism, and magnetic fabric of the Toba tuffs: constraints on the sources and eruptive styles. *J. Geophys. Res.* 91, 10355–10382.

Kozlowski, J. K. (1998). “The Middle and the Early Upper Paleolithic around the black sea,” in *Neandertals and Modern Humans in Western Asia* (New York: Plenum Press), 461–482.

Lambeck, K., and Bard, E. (2000). Sea-level change along the French Mediterranean coast for the past 30000 years. *Earth Planet. Sci. Lett.* 175, 203–222.

Langella, A., Bish, D. L., Calcaterra, D., and Cappelletti, P. (2013). “L’Ignimbrite Campana (IC),” in *Le pietre storiche della Campania dall’oblio alla riscoperta*, ed. L. Editore, 155–177.

Lee, M. Y., Chen, C. H., Wei, K. Y., Iizuka, Y., and Carey, S. (2004). First Toba supereruption revival. *Geology* 32, 61–64. doi:10.1130/G19903.1.

Lowe, J., Barton, N., Blockley, S., Ramsey, C. B., Cullen, V. L., Davies, W., et al. (2012). Volcanic ash layers illuminate the resilience of Neanderthals and early modern humans to natural hazards. *Proc. Natl. Acad. Sci.* 109, 13532–13537. doi:10.1073/pnas.1204579109.

Marianelli, P., Sbrana, A., and Proto, M. (2006). Magma chamber of the Campi Flegrei supervolcano at the time of eruption of the Campanian Ignimbrite. *Geology* 34, 937. doi:10.1130/G22807A.1.

Marti, A., Folch, A., Costa, A., and Engwell, S. (2016). Reconstructing the plinian and co-ignimbrite sources of large volcanic eruptions: A novel approach for the Campanian Ignimbrite. *Sci. Rep.* 6, 21220. doi:10.1038/srep21220.

Mason, B. G., Pyle, D. M., and Oppenheimer, C. (2004). The size and frequency of the largest explosive eruptions on Earth. *Bull. Volcanol.* 66, 735–748. doi:10.1007/s00445-004-0355-9.

McCoy, F.W., and Cornell, W. (1990). Volcaniclastic sediments in the Tyrrhenian basin. In K.A. Kastens and J. Mascle et al. (eds.) “Proceedings of the ODP”, 291-305. Scientific Results 107.

Melekestsev, I. V., Kirianov, V. Y., and Praslov, N. D. (1984). Catastrophic eruption in the Phlegrean Fields region (Italy) - possible source for a volcanic ash in late Pleistocene sediments on the European part of the USSR. *Vulcanol. i Seismol.* 3, 35–44.

Melluso, L., Morra, V., Perrotta, A., Scarpati, C., and Adabbo, M. (1995). The eruption of the Breccia Museo (Campi Flegrei, Italy): Fractional crystallization processes in a shallow, zoned magma chamber and implications for the eruptive dynamics. *J. Volcanol. Geotherm. Res.* 68, 325–339. doi:10.1016/0377-0273(95)00020-5.

Milia, A., and Torrente, M. M. (2007). The influence of paleogeographic setting and crustal subsidence on the architecture of ignimbrites in the Bay of Naples (Italy). *Earth Planet. Sci. Lett.* 263, 192–206. doi:10.1016/j.epsl.2007.08.004.

Morgan, L. A., Doherty, D. J., and Leeman, W. P. (1984). Ignimbrites of the eastern Snake river plain: evidence for major caldera-forming eruptions. *J. Geophys. Res.* 89, 8665–8678.

Mormone, A., Troise, C., Piochi, M., Balassone, G., Joachimski, M., and De Natale, G. (2015). Mineralogical, geochemical and isotopic features of tuffs from the CFDDP drill hole: Hydrothermal activity in the eastern side of the Campi Flegrei volcano (southern Italy). *J. Volcanol. Geotherm. Res.* 290, 39–52. doi:10.1016/j.jvolgeores.2014.12.003.

Narcisi, B. (1996). Tephrochronology of a late quaternary lacustrine record from the Monticchio maar (Vulture volcano, southern Italy). *Quat. Sci. Rev.* 15, 155–165. doi:10.1016/0277-3791(95)00045-3.

Narcisi, B., and Vezzoli, L. (1999). Quaternary stratigraphy of distal tephra layers in the Mediterranean - An overview. *Glob. Planet. Change* 21, 31–50. doi:10.1016/S0921-8181(99)00006-5.

Newhall, C. G., and Self, S. (1982). The volcanic explosivity index (VEI) an estimate of explosive magnitude for historical volcanism. *J. Geophys. Res.* 87, 1231. doi:10.1029/jc087ic02p01231.

Orsi, G., De Vita, S., and Di Vito, M. A. (1996). The restless, resurgent Campi Flegrei nested caldera (Italy): constraints on its evolution and configuration. *J. Volcanol. Geotherm. Res.* 74, 179–214.

Ort, M. H., Orsi, G., Pappalardo, L., and Fisher, R. V. (2003). Anisotropy of magnetic susceptibility studies of depositional processes in the Campanian Ignimbrite , Italy. *Bull. Volcanol.* 65, 55–72. doi:10.1007/s00445-002-0241-2.

Ortolani, F., and Aprile, F. (1985). Principali caratteristiche stratigrafiche e strutturali dei depositi superficiali della piana campana. *Boll. Soc. Geol. It.* 104, 195–206.

Pacheco-Hoyos, J. G., Aguirre-Díaz, G. J., and Dávila-Harris, P. (2018). Boiling-over dense pyroclastic density currents during the formation of the ~ 100 km3 Huichapan ignimbrite in Central Mexico: Stratigraphic and lithofacies analysis. *J. Volcanol. Geotherm. Res.* 349, 268–282. doi:10.1016/j.jvolgeores.2017.11.007.

Pappalardo, L., Civetta, L., D'Antonio, M., Deino, A. L., Di Vito, M. A., Orsi, G., et al. (1999). Chemical and Sr-isotopical evolution of the Phlegraean magmatic system before the Campanian Ignimbrite and the Neapolitan Yellow Tuff eruptions. *J. Volcanol. Geotherm. Res.* 91, 141–166. doi:10.1016/S0377-0273(99)00033-5.

Pappalardo, L., Ottolini, L., and Mastrolorenzo, G. (2008). The Campanian Ignimbrite (southern Italy) geochemical zoning: Insight on the generation of a super-eruption from catastrophic differentiation and fast withdrawal. *Contrib. to Mineral. Petrol.* 156, 1–26. doi:10.1007/s00410-007-0270-0.

Parfitt, L., and Wilson, L. (2008). *Fundamentals of Physical Volcanology*. Malden, USA: Blackwell.

Parker, D. F., and McDowell, F. W. (1979). K-Ar geochronology of Oligocene volcanic rocks , Davis and Barrilla Mountains , Texas. *Geol. Soc. Am. Bull.* 90, 1100–1110.

Paterne, M. (1992). "Additional remarks on tephra layer from Temnata Cave," in *Temnata Cave. Excavations in Karlukovo Karst Area, Bulgaria,* eds. J. K. Kozlowski, H. Laville, and B. Ginter, 99–100.

Paterne, M., Guichard, F., and Labeyrie, J. (1988). Explosive activity of the South Italian volcanoes during the past 80,000 years as determined by marine tephrochronology. *J. Volcanol. Geotherm. Res.* 34, 153–172. doi:10.1016/0377-0273(88)90030-3.

Paterne, M., Guichard, F., Labeyrie, J., Gillot, P. Y., and Duplessy, J. C. (1986). Tyrrhenian Sea tephrochronology of the oxygen isotope record for the past 60,000 years. *Mar. Geol.* 72, 259–285. doi:10.1016/0025-3227(86)90123-4.

Paterne, M., Kallel, N., Labeyrie, L., Vautravers, M., Duplessy, J. C., Rossignol-Strick, M., et al. (1999). Hydrological relationship between the North Atlantic Ocean and the Mediterranean Sea during the past 15 - 75 kyr. *Paleoceanography* 14, 626–638. doi:10.1029/1998PA900022.

Pérez, W., Alvarado, G. E., and Gans, P. B. (2006). The 322 ka Tiribí Tuff: Stratigraphy, geochronology and mechanisms of deposition of the largest and most recent ignimbrite in the Valle Central, Costa Rica. *Bull. Volcanol.* 69, 25–40. doi:10.1007/s00445-006-0053-x.

Perrotta, A., and Scarpati, C. (1994). The dynamics of the Breccia Museo eruption (Campi Flegrei, Italy) and the significance of spatter clasts associated with lithic breccias. *J. Volcanol. Geotherm. Res.* 59, 335–355. doi:10.1016/0377-0273(94)90086-8.

Perrotta, A., and Scarpati, C. (2003). Volume partition between the plinian and co-ignimbrite air fall deposits of the Campanian Ignimbrite eruption. *Mineral. Petrol.* 79, 67–78. doi:10.1007/s00710-003-0002-8.

Perrotta, A., Scarpati, C., Luongo, G., and Morra, V. (2006). Chapter 5 The Campi Flegrei caldera boundary in the city of Naples. *Dev. Volcanol.* 9, 85–96. doi:10.1016/S1871-644X(06)80019-7.

Perrotta, A., Scarpati, C., Luongo, G., and Morra, V. (2010). Stratigraphy and volcanological evolution of the southwestern sector of Campi Flegrei and Procida Island , Italy. *Geol. Soc. Am. Spec. Pap.* 80301, 171–191. doi:10.1130/2010.2464(09).

Piochi, M., Mastrolorenzo, G., and Pappalardo, L. (2005). Magma ascent and eruptive processes from textural and compositional features of Monte Nuovo pyroclastic products, Campi Flegrei, Italy. *Bull. Volcanol.* 67, 663–678. doi:10.1007/s00445-005-0410-1.

Pyle, D. M. (1989). The thickness, volume and grainsize of tephra fall deposits. *Bull. Volcanol.* 51, 1–15.

Pyle, D. M. (1990). "New volume estimates for the Minoan eruption of Santorini," in *Thera and the Aegean World III* (London: The Thera Foundation), 113–121.

Pyle, D. M., Ricketts, G. D., Margari, V., van Andel, T. H., Sinitsyn, A. A., Praslov, N. D., et al. (2006). Wide dispersal and deposition of distal tephra during the Pleistocene "Campanian Ignimbrite/Y5" eruption, Italy. *Quat. Sci. Rev.* 25, 2713–2728. doi:10.1016/j.quascirev.2006.06.008.

Rampino, M. R., and Self, S. (1992). Volcanic winter and accelerated glaciation following the Toba super-eruption. *Nature* 359, 50–52.

Ratté, J. C., Marvin, R. F., Naeser, C. W., and Bikerman, M. (1984). Calderas and ash flow tuffs of the Mogollon Mountains, southwestern New Mexico. *J. Geophys. Res.* 89, 8713. doi:10.1029/JB089iB10p08713.

Rolandi, G., Bellucci, F., Heizler, M. T., Belkin, H. E., and De Vivo, B. (2003). Tectonic controls on the genesis of ignimbrites from the Campanian Volcanic Zone, southern Italy. *Mineral. Petrol.* 79, 3–31. doi:10.1007/s00710-003-0014-4.

Rosi, M., and Sbrana, A. (1987). Phlegrean Fields. *CNR, Quad. La "Ricerca Sci.* 114, 1–175.

Rosi, M., Sbrana, A., and Principe, C. (1983). The phlegraean fields: Structural evolution, volcanic history and eruptive mechanisms. *J. Volcanol. Geotherm. Res.* 17, 273–288. doi:10.1016/0377-0273(83)90072-0.

Rosi, M., Sbrana, A., and Vezzoli, L. (1988). Correlazioni tefrostratigrafiche di alcuni livelli di Ischia, Procida e Campi Flegrei. *Mem. della Soc. Geol. Ital.* 41, 1015–1027.

Rosi, M., Vezzoli, L., Aleotti, P., and Censi, M. (1996). Interaction between caldera collapse and eruptive dynamics during the Campanian Ignimbrite eruption, Phlegraean Fields, Italy. *Bull. Volcanol.* 57, 541–554. doi:10.1007/BF00304438.

Rosi, M., Vezzoli, L., Castelmenzano, A., and Grieco, G. (1999). Plinian pumice fall deposit of the Campanian Ignimbrite eruption (Phlegraean Fields, Italy). *J. Volcanol. Geotherm. Res.* 91, 179–198. doi:10.1016/S0377-0273(99)00035-9.

Ruberti, D., Vigliotti, M., Rolandi, R., and Di Lascio, M. (2020). "Effect of paleomorphology on facies distribution of the Campania Ignimbrite in the northern Campania Plain, southern Italy," in *Vesuvius, Campi Flegrei, and Campanian Volcanism* (Elsevier Inc.), 207–229. doi:10.1016/B978-0-12-816454-9.00009-2.

Sbrana, A., and Toccaceli, R. M. (2011). Carta Geologica della Regione Campania in scala 1: 10.000, Foglio 464 Isola d'Ischia.

1050 Scandone, R., Bellucci, F., Lirer, L., and Rolandi, G. (1991). The structure of the Campanian Plain
1051 and the activity of the Neapolitan volcanoes (Italy). *J. Volcanol. Geotherm. Res.* 48, 1–31.
1052 doi:10.1016/0377-0273(91)90030-4.

1053 Scarpati, C., and Perrotta, A. (2012). Erosional characteristics and behavior of large pyroclastic
1054 density currents. *Geology* 40, 1035–1038. doi:10.1130/G33380.1.

1055 Scarpati, C., and Perrotta, A. (2016). Stratigraphy and physical parameters of the Plinian phase of the
1056 Campanian Ignimbrite eruption. *Bull. Geol. Soc. Am.* 128, 1147–1159. doi:10.1130/B31331.1.

1057 Scarpati, C., Perrotta, A., Lepore, S., and Calvert, A. (2013). Eruptive history of Neapolitan
1058 volcanoes : constraints from 40 Ar – 39 Ar dating. *Geol. Mag.* 150, 412–425.
1059 doi:10.1017/S0016756812000854.

1060 Scarpati, C., Sparice, D., and Perrotta, A. (2014). A crystal concentration method for calculating
1061 ignimbrite volume from distal ash-fall deposits and a reappraisal of the magnitude of the
1062 Campanian Ignimbrite. *J. Volcanol. Geotherm. Res.* 280, 67–75.
1063 doi:10.1016/j.jvolgeores.2014.05.009.

1064 Scarpati, C., Sparice, D., and Perrotta, A. (2015a). Facies variation in the Campanian Ignimbrite.
1065 *Rend. Online Soc. Geol. Ital.* 33, 83–87. doi:10.3301/ROL:2015.20.

1066 Scarpati, C., Sparice, D., and Perrotta, A. (2015b). The ground layer of the Campanian Ignimbrite: an
1067 example of deposition from a dilute pyroclastic density current. *Bull. Volcanol.* 77.
1068 doi:10.1007/s00445-015-0985-0.

1069 Servizio Geologico d'Italia (1963). Carta geologica d'Italia scala 1:100.000, foglio 174 – Ariano
1070 Irpino "Geological map of Italy at 1:100.000 scale, sheet number 174 – Ariano Irpino". Servizio
1071 Geologico d'Italia, Rome.

1072 Servizio Geologico d'Italia (1965a). Carta geologica d'Italia scala 1:100.000, foglio 185 – Salerno
1073 "Geological map of Italy at 1:100.000 scale, sheet number 185 – Salerno". Servizio Geologico
1074 d'Italia, Rome.

1075 Servizio Geologico d'Italia (1965b). Carta geologica d'Italia scala 1:100.000, foglio 196 – Sorrento
1076 "Geological map of Italy at 1:100.000 scale, sheet number 196 – Sorrento". Servizio Geologico
1077 d'Italia, Rome.

1078 Servizio Geologico d'Italia (1965c). Carta geologica d'Italia scala 1:100.000, foglio 197 – Amalfi
1079 "Geological map of Italy at 1:100.000 scale, sheet number 197 – Amalfi". Servizio Geologico
1080 d'Italia, Rome.

1081 Servizio Geologico d'Italia (1966). Foglio Geologico n°172 - Caserta. Carta Geologica d'Italia, scala
1082 1:100.000, II ediz., Istituto Poligrafico e Zecca dello Stato, Roma.

1083 Servizio Geologico d'Italia (1967a). Carta geologica d'Italia scala 1:100.000, fogli 183-184 – Isola di
1084 Ischia – Napoli "Geological map of Italy at 1:100.000 scale, sheet number 183-184 – Isola di
1085 Ischia - Napoli". Servizio Geologico d'Italia, Rome.

1086 Servizio Geologico d'Italia (1967b). Carta geologica d'Italia scala 1:100.000, fogli 160 – Cassino

"Geological map of Italy at 1:100.000 scale, sheet number 160 – Cassino". Servizio Geologico d'Italia, Rome.

Servizio Geologico d'Italia (1971a). Carta geologica d'Italia scala 1:100.000, foglio 171 – Gaeta e Vulcano di Roccamonfina "Geological map of Italy at 1:100.000 scale, sheet number 171 – Gaeta e Vulcano di Roccamonfina". Servizio Geologico d'Italia, Rome.

Servizio Geologico d'Italia (1971b). Carta geologica d'Italia scala 1:100.000, foglio 161 – Isernia "Geological map of Italy at 1:100.000 scale, sheet number 161 – Isernia". Servizio Geologico d'Italia, Rome.

Servizio Geologico d'Italia (1975). Carta geologica d'Italia scala 1:100.000, foglio 173 – Benevento "Geological map of Italy at 1:100.000 scale, sheet number 173 – Benevento". Servizio Geologico d'Italia, Rome.

Seymour, K. S., and Christanis, K. (1995). Correlation of a tephra layer in western greece with a late pleistocene eruption in the campanian province of italy. *Quat. Res.* 43, 46–54. doi:10.1006/qres.1995.1005.

Seymour, K. S., Christanis, K., Bouzinos, A., Papazisimou, S., Papatheodorou, G., Moran, E., et al. (2004). Tephrostratigraphy and tephrochronology in the Philippi peat basin, Macedonia, Northern Hellas (Greece). *Quat. Int.* 121, 53–65. doi:10.1016/j.quaint.2004.01.023.

Smith, R. L. (1960). Ash flows. *Bull. Geol. Soc. Am.* 71, 795–841. doi:10.1130/0016-7606(1960)71[795:AF]2.0.CO;2.

Smith, V. C., Isaia, R., Engwell, S., and Albert, P. G. (2016). Tephra dispersal during the Campanian Ignimbrite (Italy) eruption: implications for ultra-distal ash transport during the large caldera-forming eruption. *Bull. Volcanol.* 78. doi:10.1007/s00445-016-1037-0.

Smith, V. C., Isaia, R., and Pearce, N. J. G. (2011). Tephrostratigraphy and glass compositions of post-15 kyr Campi Flegrei eruptions: Implications for eruption history and chronostratigraphic markers. *Quat. Sci. Rev.* 30, 3638–3660. doi:10.1016/j.quascirev.2011.07.012.

Sparice, D. (2015). Definizione delle litofacies e ricostruzione dell'architettura dell'Ignimbrite Campana.

Sparks, R. S. J., Francis, P. W., Hamer, R. D., Pankhurst, R. J., O'Callaghan, L. O., Thorpe, R. S., et al. (1985). Ignimbrites of the Cerro Galan caldera, NW Argentina. *J. Volcanol. Geotherm. Res.* 24, 205–248.

Sparks, R. S. J., and Huang, T. C. (1980). The volcanological significance of deep-sea ash layer associated with ignimbrites. *Geol. Mag.* 117, 425–436.

Sparks, R. S. J., and Walker, G. P. L. (1977). The significance of vitric-enriched air-fall ashes associated with crystal-enriched ignimbrites. *J. Volcanol. Geotherm. Res.* 2, 329–341.

Sparks, S., Self, S., Grattan, J., Oppenheimer, C., Pyle, D. M., and Rymer, H. (2005). Super-eruptions: global effects and future threats. London.

Stuiver, M., Grootes, P. M., and Braziunas, T. F. (1995). The GISP2 □18O Climate Record of the Past 16,500 Years and the Role of the Sun, Ocean, and Volcanoes. *Quat. Res.* 44, 341–354.

Tanguy, J. C., Ribière, C., Scarth, A., and Tjetjep, W. S. (1998). Victims from volcanic eruptions: a revised database. *Bull. Volcanol.* 60, 137–144. doi:10.1007/s004450050222.

Thordarson, T., and Self, S. (1996). Sulfur, chlorine and fluorine degassing and atmospheric loading by the Roza eruption, Columbia River Basalt Group, Washington, USA. *J. Volcanol. Geotherm. Res.* 74, 49–73.

Thunell, R., Federman, A., Sparks, R. S. J., and Williams, D. (1979). The age, origin, and volcanological significance of the Y-5 ash layer in the Mediterranean. *Quat. Res.* 12, 241–253. doi:10.1016/0033-5894(79)90060-7.

Ton-That, T., Singer, B., and Paterne, M. (2001). 40Ar/39 dating of latest Pleistocene (41 ka) marine tephra in the Mediterranean sea: Implications for global climate records. *Earth Planet. Sci. Lett.* 184, 645–658. doi:10.1016/S0012-821X(00)00358-7.

Torrente, M. M., Milia, A., Bellucci, F., and Rolandi, G. (2010). Extensional tectonics in the Campania Volcanic Zone (eastern Tyrrhenian Sea , Italy): New insights into the relationship between faulting and ignimbrite eruptions. *Boll. Soc. Geol. It.* 129, 297–315. doi:10.3301/IJG.2010.07.

Upton, J., Cole, P. D., Shaw, P., Szakacs, A., and Seghedi, I. (2002). "Correlation of tephra layers found in southern Romania with the Campanian Ignimbrite (~37 ka)," in *The Quaternary Research Association and First Postgraduate Paleo-environmental Symposium* (Amsterdam: Universiteit van Amsterdam).

Veres, D., Lane, C. S., Timar-Gabor, A., Hambach, U., Constantin, D., Szakács, A., et al. (2013). The Campanian Ignimbrite/Y5 tephra layer - A regional stratigraphic marker for Isotope Stage 3 deposits in the Lower Danube region, Romania. *Quat. Int.* 293, 22–33. doi:10.1016/j.quaint.2012.02.042.

Vezzoli, L. (1991). Tephra layers in Bannock Basin (Eastern Mediterranean). *Mar. Geol.* 100, 21–34. doi:10.1016/0025-3227(91)90221-O.

Vezzoli, L., and Barberi, F. (1988). Progetto finalizzato geodinamica: monografie finali. X: Island of Ischia. *Quad. La Ric. Sci.* 114.

Vitale, S., and Isaia, R. (2014). Fractures and faults in volcanic rocks (Campi Flegrei, southern Italy): Insight into volcano-tectonic processes. *Int. J. Earth Sci.* 103, 801–819. doi:10.1007/s00531-013-0979-0.

Vitaliano, C. J., Taylor, S. R., Farrand, W. R., and Jacobsen, T. W. (1981). "Tephra layer in Franchthi Cave, Peleponnesos, Greece," in *Tephra studies* (Dordrecht: Springer), 373–379.

Walker, G. P. L. (1972). Crystal concentration in ignimbrites. *Contrib. to Mineral. Petrol.* 36, 135–146. doi:10.1007/BF00371184.

Walker, G. P. L. (1980). The Taupo pumice: product of the most powerful known (ultraplinian)

eruption? *J. Volcanol. Geotherm. Res.* 8, 69–94.

Walker, G. P. L. (1981). Characteristics of two phreatoplinian ashes, and their water-flushed origin. *J. Volcanol. Geotherm. Res.* 9, 395–407. doi:10.1016/0377-0273(81)90046-9.

Walker, G. P. L. (1983). Ignimbrite types and ignimbrite problems. *J. Volcanol. Geotherm. Res.* 17, 65–88.

Wilson, C. J. N. (2001). *The 26.5 ka Oruanui eruption, New Zealand: An introduction and overview*. doi:10.1016/S0377-0273(01)00239-6.

Wilson, C. J. N., and Walker, G. P. L. (1985). The Taupo eruption, New Zealand. 1. General aspects. *Philos. Trans. R. Soc. A Math. Phys. Eng. Sci.* 314, 199–228.

Witham, C. S. (2005). Volcanic disasters and incidents: A new database. *J. Volcanol. Geotherm. Res.* 148, 191–233. doi:10.1016/j.jvolgeores.2005.04.017.

Woods, A. W. (1998). Observations and models of volcanic eruption columns. *Geol. Soc. Spec. Publ.* 145, 91–114. doi:10.1144/GSL.SP.1996.145.01.06.

Woods, A. W., and Wohletz, K. (1991). Dimensions and dynamics of co-ignimbrite eruption columns. *Nature* 350, 225–227. doi:10.1038/350225a0.

Wulf, S., Kraml, M., Brauer, A., Keller, J., and Negendank, J. F. W. (2004). Tephrochronology of the 100ka lacustrine sediment record of Lago Grande di Monticchio (southern Italy). *Quat. Int.* 122, 7–30. doi:10.1016/j.quaint.2004.01.028.

10 Data Availability Statement

The datasets generated and analyzed for this study can be found in the Data Repository https://mfr.osf.io/render?url=https%3A%2F%2Fosf.io%2F3a6bz%2Fdownload. QGIS data are available on request to the corresponding author.